REPUBLIC OF THE PHILIPPINES

OFFSHORE MINERAL RESOURCES IN THE PHILIPPINES

SURVEY REPORT

JANUARY 1971

Prepared for
Overseas Technical Cooperation Agency
Government of Japan
by Japanese Survey Team for
Philippines Offshore Mineral
Resourses Project

REPUBLIC OF THE PHILIPPINES

OFFSHORE MINERAL RESOURCES IN THE PHILIPPINES

SURVEY REPORT

JANUARY 1971

Prepared for
Overseas Technical Cooperation Agency
Government of Japan
by Japanese Survey Team for
Philippines Offshore Mineral
Resourses Project

PREFACE

In compliance with the request from the government of the Philippines, the Government of Japan decided to undertake a survey on mineral resources in the coastal areas and littoral districts mainly on the south-eastern Ruzon in the Philippines. For this purpose, the government of Japan entrusted the Overseas Technical Cooperation Agency (OTCA) with the execution of the aforementioned survey.

The chief objective of this survey is to carry out geological investigations so as to make studies on the possibility of developing mineral resources by conducting aero-magnetic surveys.

Hence, OTCA organized a survey team composed of eleven members, headed by Dr. Shunichi Sano, Senior Researcher of Geological Survey of Japan, Ministry of International Trade and Industry and dispatched the team to the Philippines for a period of 34 days from February 25 through March 30, 1970 with the aim of investigating subsurface structures covering 18,500 km^2, especially the thickness of sediments and configuration of their Mozoic basements from the coastal districts on the southern Ruzon to the offing south of the Mindoro Island.

After returning to Tokyo, the team has directed its efforts to the compilation and analysis of data and materials collected during the field survey, and the results are hereby submitted to the government of the Philippines.

It is my sincere hope that the report will be of great help to the progress of development of mineral resources in the Philippines thereby contributing to the advancement of her national economy and to further strengthening the bond of friendship and goodwill between the two nations.

In closing, on behalf of OTCA, I would like to express my heartfelt appreciation to the government of the Philippines for its full cooperation and assistance extended to the team during the course of the field studies.

January 1971

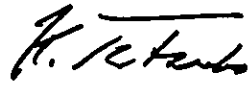

Keiichi Tatsuke
Director General
Overseas Technical Cooperation Agency

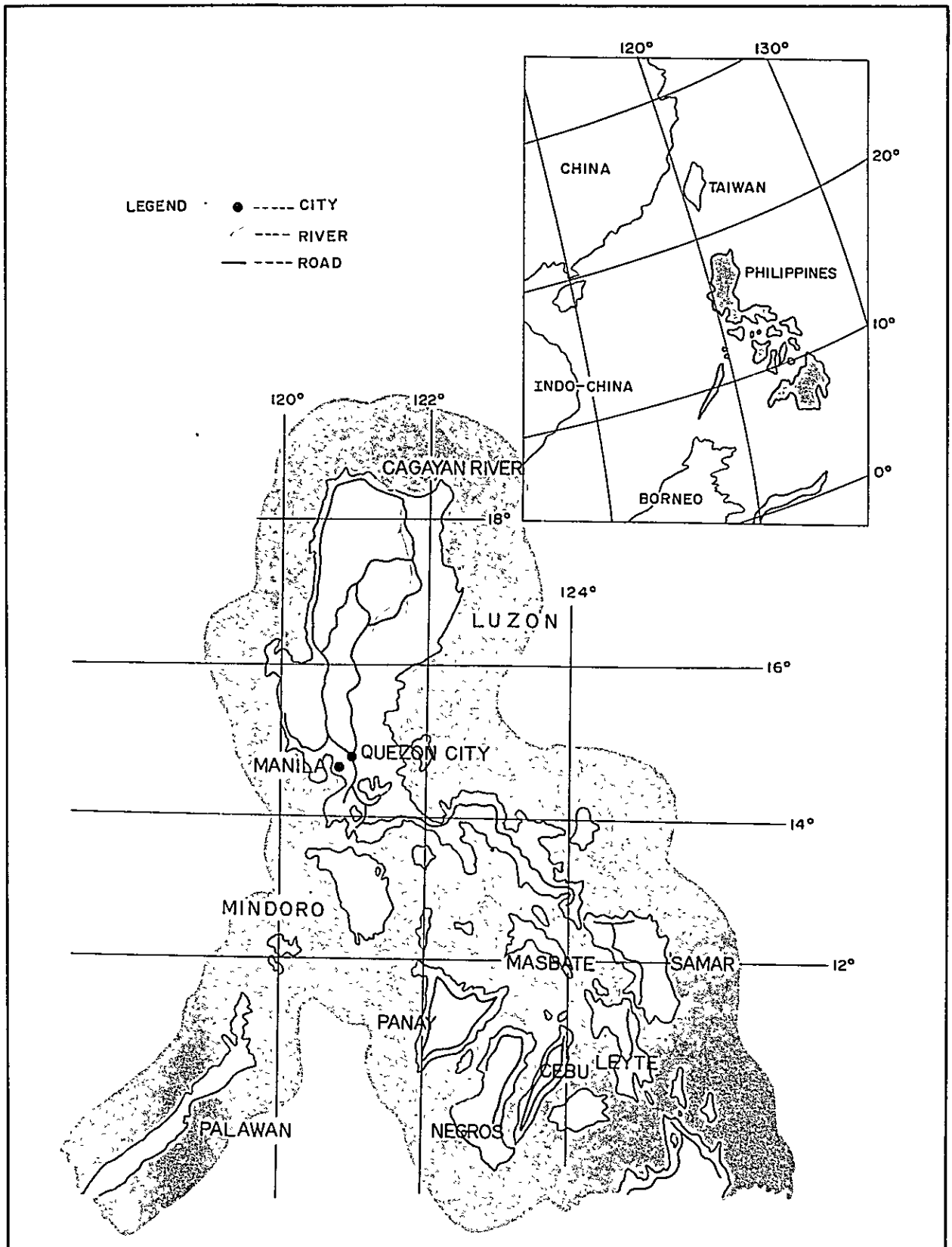

Key Map & Location Map

CONTENTS

PAGE

I. INTRODUCTION

I-1. Background

At the first session of the Committee for Co-ordination of Joint-Prospecting for Mineral Resources in Asian Offshore Areas (CCOP) held in Quezon City in May-June, 1966, the government of the Philippines proposed to CCOP an aeromagnetic survey plan covering nearly the whole territory as a joint survey project of the Committee, the territory being devided into six parts, namely Region I to Region VI, from the viewpoint of petroleum exploration. The possibility of the assistance for a limited aeromagnetic survey was offered by the government of Japan at the third session of CCOP held in Seoul in June-July, 1967 and it was recommended at the fourth session of CCOP held in Taipei in November, 1967 that the offer should be allocated to the aeromagnetic survey in the part of Region II of the Plan. The proposed aeromagnetic survey was included in the work programme of CCOP as project CCOP-1/PH.2.

At the request of the government of the Philippines, the government of Japan sent an expert team consisting of two gelolgists and a geophysicist to make preliminary survey arrangements and to collect geologic data of the projected area in March and April of 1968. The survey plan prepared by this expert team, based on the original proposal made by the Philippine Bureau of Mines, was submitted for discussion at the fifth session of CCOP held in Tokyo in June, 1968. However, this project was not realized for more than a year after the fifth session.

During the Fourth Regional Symposium on Development of Petroleum Resources in Asia and the Far East held at Camberra in October 1969, the Philippine delegation called to the attention of the Japanese delegation as well as of the ECAFE Secretariat the advisability of undertaking of the project. After that meeting the government of the two countries concerned were notified of the results of the discussions including those made at the previous sessions of CCOP and thereafter the two governments confirmed the agreement for the implementation of assistance to

be rendered by the government of Japan and the counterparts to be borne by the government of the Philippines.

The government of Japan, subsequently, entrusted the execution of the project to the Overseas Technical Cooperation Agency and the survey team was organized and dispatched to the Philippines by this Agency.

The original area was a rectangle extending in a northwest-southwest direction by about 400 km, having a width of about 40 km and covered parts of Southern Luzon, Marinduque and Mindoro Islands and their offshore areas. As shown in the location map (Fig. 1) and mentioned hereafter, some revisions were made during the actual survey to facilitate flight operations.

The government of Japan provided the survey team consisting of geophysicists, engineers, pilots, mechanics and secretaries as well as the necessary equipment and a survey aircraft. The necessary counterparts were borne or provided for by the government of the Philippines, as follows:

1. Fuel (13,001 U.S. galons) and refueling facilities.
2. Customs clearance of the equipment and the aircraft.
3. Waiver of landing charge and parking fee of the aircraft.
4. Ground handling of the aircraft.
5. Security of the equipments and the aircraft.
6. Dark room and copy machine space in the Bureau of Mines.
7. Car with a driver.
8. Waiting room at the airport.
9. Observation room for station magnetometer.
10. Airphotos of the projected area.
11. Counterpart personnel from the Bureau of Mines:
    liaison officer, geologist, ground magnetometer operator and copy machine operator.

The processing, reduction and geologic interpretation of the magnetic data were made at the Geological Survey of Japan. The government of the Philippines sent a geologist from its Bureau of Mines to participate in these office works from July 1, 1970 to September 30, 1970, especially in the interpretation of the aeromagnetic data as correlated with the surface geology of the areas traversed by the survey. This participation was made possible at the expense of the government of Japan.

I-2. Objectives of the Survey

The aeromagnetic survey was planned as a reconnaissance for the revelation of the mineral potentiality of the area, by determining the thickness of the sediments overlying Mesozoic basement and detecting subsurface structures favourable for the occurence of mineral resources, including petroleum. In Marinduque Island of the area surveyed, several copper mines are under development and production. In Bondoc Peninsula adjacent to the surveyed area, indications of the existance of natural gas have been reported. Additional metallic mineral deposits as well as accumulations of hydrocarbons on land and offshore are expected to be discovered.

The flight pattern of the survey was somewhat modified during the operation mainly due to the weather conditions in the area. Curved traverse lines parallel with Loran-A lines of position were originally proposed by the Japanese team, but this plan was discarded soon after the test flight because it was found that propagation of Loran-A waves was greatly distorted over land areas. Accordingly, six straight traverses of more than 350 km each in length were flown in a northeast-southwest direction with a spacing of about 6 km, although some parts of the traverses remained unflown due to unfavourable weather conditions. The northern half of the projected area was extended northwestward since preliminary magnetic profiles suggested the existence of a sedimentary basin beneath Lamon Bay, north of Alabat Island. Eight short traverses of about 150 km long were additionally flown with a spacing of about 6 km. Five tie lines from 50 to 100 km in length were also completed. The traverses were successively numbered from #1 to #14 northwestward and the tie lines from p2 to p6 southwestward.

Subsequently, the total length of traverses was 3,800 line-km excluding ref-light of 200 km, while the total tie line length was 400 line-km. The total flight length was thus 4,200 line-km that covered an area of about 18,500 sq.km. The flight level was maintained at 3,000 ft above sea level except over the mountaneous part of Mindoro. The air speed of aircraft was about 140 mph.

I-3. Organization of the Team

The members of the survey team dispatched to the Philippines were as follows:

Name	Position	Organization
Dr. Shun-ichi Sano	Head	Geological Survey of Japan, Ministry of International Trade and Industry (MITI)
Mr. Kunio Hiraki	Liaison Officer	Nippon Air-Transport Company (NATC)
Mr. Yoshio Tamura	Geophysicist	Geological Survey of Japan, MITI
Mr. Katsuro Ogawa	Geophysicist	Geological Survey of Japan, MITI
Mr. Yasumichi Iijima	Electronic Engineer	Marubun Company
Mr. Seiji Nakagawa	Surveyer	Sumiko Consultant Company
Mr. Hironao Suzuki	Co-ordinator	Overseas Technical Cooperation Agency
(Flight Crew)		
Mr. Motoji Ichikawa	Captain	NATC
Mr. Takeshi Sakabe	Co-pilot	NATC
Mr. Toshio Tateishi	Mechanics	NATC
Mr. Hiromichi Kizaki	Mechanics	NATC

The survey team arrived at Manila on March 4, 1970 and left Manila on March 29, 1970. The Head and the Liaison Officer of the team left Tokyo in advance on February 26th for Taipei, Republic of China in order to obtain the landing permission of the survey aircraft at Taipei International Airport and arrived in Manila on February 27th. The Liaison Officer left Manila on March 10th after completing his duty. The survey aircraft, a YS-11 prop-jet passenger plane converted for aerial surveys and equiped with survey instruments took off from Tokyo on March 3rd and landed in Manila on March 4th after staying overnight in Taipei. The aircraft left Manila on March 29th and returned to Tokyo on March 30th via Taipei after completion of the survey flights.

I-4. Acknowledgements

Mr. Felipe U. Francisco, Chief of the Petroleum Division, Bureau of Mines and Mr. Carlos F. Teodoro, Supervising Geologist of the Division were in charge of the arrangements for counterparts throughout the field operation and discussed with the Japanese team amendments of the survey plan as the field operations progressed. The following personnel of the Bureau of Mines also actively co-operated in the field operation:

Mr. Dominador Muriel	Liaison Officer
Mr. Pedro Estupigan	Geologist
Mr. Juan de la Cruz	Geologist in charge of the operation of ground magnetometer and office machines
Mr. Herminio Taquiqui	Surveyer in charge of the operation of ground magnetometer.

Mr. D. Muriel, Supervising Geologist of the Petroleum Division participated also in the geologic interpretation and the preparation of the report..

The Japanese survey team wishes to express its sincere gratitude to the Bureau of Mines and its personnel for their co-operative efforts and assistance throughout the field operation and also to the Philippine Air Force as well as to the Civil Aeronautics Adiministration for their assistance in the flight operation. Thanks are also due to the Weather Bureau for providing a suitable site for the station magnetometer and to the Coast and Geodetic Survey for providing the results of the continuous geomagnetic observation.

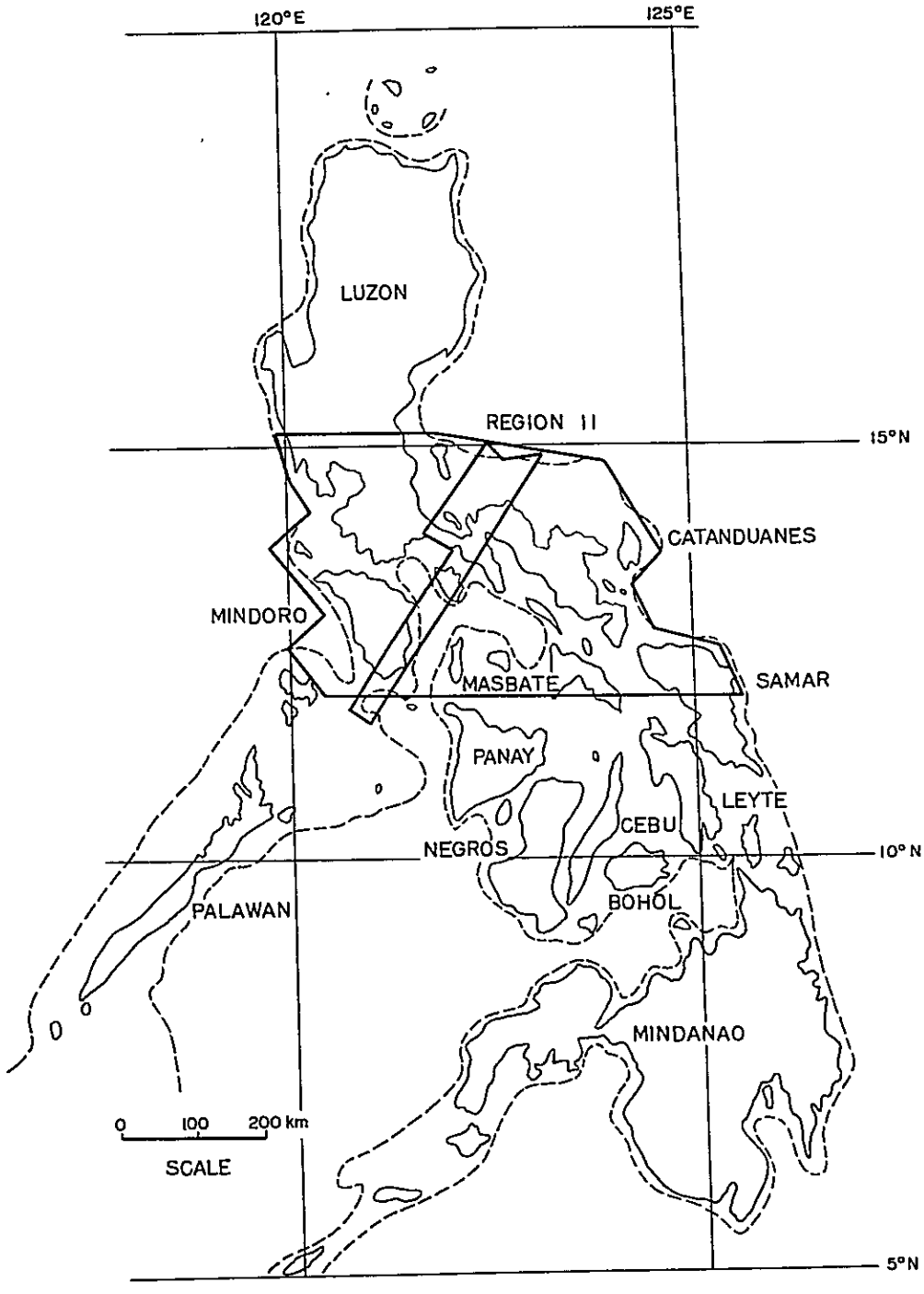

Fig. 1 Location Map

II. OUTLINE OF GEOLOGY

Although many papers on the regional and local geology of the Philippines have been published (for example, Alcarez, 1947: Corby et al., 1951: Gervasio, 1966a, 1966b: Santos-Ynigo, 1966, for general geology of the Philippines), the latest available geological map is the map series at scale of 1:1,000,000 alone issued by the Bureau of Mines (1963). The geologic interpretation was conducted based on this geologic sheet map. The following explanation on geology on land is summerized mainly from an unpublished report prepared by the Petroleum Division, Bureau of Mines (1970). This report does not include the description on the geology of southern Luzon besides Camarines Norte.

II-1. Southern Mindoro

The oldest rocks in the area are metamorphic rocks consisting mainly of schists, slates and gneisses. These metamorphic rocks are found in abundance along the Wasig river in the south and extending northward direction. In some places the bedding structures are still preserved but in others the structure may have been developed by metamorphic processes.

The ammonite-bearing Manslay formation consists principally of conglomerate, black shales, cherts, graywackes and lignitic materials. The first well preserved ammonite was discovered in this area and subsequently in other places to the north and south of the district. These sedimentary rocks were deposited discordantly on top of the crystalline basement rocks (Feliciano and Basco, 1947).

The Cretaceous period was characterized by intrusions of igneous rocks and thrusting of serpentinized ultrabasic rocks. It seems that the igneous rocks intruded the Mansalay formation causing alterations around the periphery. Except for some silicification the dark shales seem to be slightly affected by the intrusion of the igneous rocks probably because of the impermeability and resistant physical property of the shales. The diorite is highly altered but when fresh it contains visible feldspars

and ferromagnesian minerals.

During Eocene time, limestone and carbonaceous clastics were deposited probably without interruption. The basal conglomerate is composed of well cemented pebbles of diorite, gabbro, black shales, gneisses and other materials derived from older rocks. The limestone outcrops appear as well-bedded patches on topographic highs and along the slopes north and south of the town of Mansalay. The clastic sediments are largely wackes and shales, sometimes closely associated with conglomerate.

Oligocene-Miocene limestones interbedded with shales, sandstones and silts occupy the southern part of the area extending up to Semirara Island. It is gently folded and well bedded. In many places, evidence of recrystallization was noted. It is light gray to white in colour but pinkish when weathered. Calcareous nodules enclosed in the silt layers record the presence of algae zones. A considerable amount of light-gray sandstone is interbedded with limestone in the lower part of the formation. Generally, it is fine grained but some layers are conglomeratic. In some areas, light to dark grey shales are developed rather than coarser silty materials and some parts are calcareous and fossiliferous. This part includes several coal measures (Weller and Vergara, 1955).

Areas subjected to recent uplift contain deposits of alluvium, reefal limestone and terrace gravel. Poorly consolidated conglomerates were deposited on low areas but they are insignificant in extent.

In general, the structures in the region are predominantly northwest-southeast trending thrust faults and flexural folds.

II-2. Marinduque Island

The oldest rock formation exposed on this island consists of undifferentiated metamorphosed volcanic rocks and graywackes with small bodies of serpentine. This overlained by a series of altered sandstone, shale and marble with thin layer of dacite and/or andesite flows. Outcrops of this Eocene formation are exposed along a northwest-southeast trending belt in the central part of the island.

The Eocene formation is a uncontormably overlain by a thick sequence of andesitic flows. The major part of the sequence is exposed along the northeast flank of the island. At the southwestern side, these rocks are highly fractured due to later tectonic activities. Above this andesitic flows are thin chert beds which are found in patches as cappings on prominent peaks on the northeastern flank.

Unconformably overlying the volcanic flows are lenses of Middle Miocene reef limestone occasionally interbedded with basaltic flows and pyroclastics. Some degree of crystallization of the Middle Miocene limestones has taken place near the diorte bodies. The basal section of the Middle Miocene formation was invaded by criss-crossing andesite porphyry dikes. Thick tuffaceous sedimentary rocks overlie the Middle Miocene formation along the western flank and a few outcrops are also present on the northeastern side of the island. The beds are folded into syncliness and anticliness.

Unconformably above the tuffaceous formation are fine pyroclastic sediments. Mineralogical study of these sediments show that they have resulted from reworking of the tuff. These sediments are fossiliferous and dated Mio-Pliocene. The beds in some areas dip gently to the southwest. Occasional terrace gravel along the west coast near Boac, indicate that intermittent uplift is still active.

At the southernmost part of the island is the dormant volcano known as Mt. Malindig; along its slopes are fragmental volcanic rocks of intermediate to basic composition which cover both the basal metamorphic formation and lenses of Middle Miocene limestone and tuff. Quaternary alluvium was deposited along the valley follrs.

The most prominent fractures are oriented northwest-southeast also parallel to the Philippine Rift Zone. This is exemplified by the areal distribution and elongation of the plutonic bodies. It is probable that the emplacement of these plutonic bodies was guided by northwest-southeast fractures and the surrounding rocks were worped into a broad anticlinal pattern (Gervasio, 1958: Irving, 1950: Santos-Ynigo, 1959).

II-3. Paracale Mineral District, Camarines Norte, Southern Luzon

The oldest rock types exposed in the offshore islets of Camarines Norte consist of parashists and orthoschists belonging to a higher grade of metamorphism. At Larap peninsula, lower grade metamorphic rocks occur. These rocks are principally chlorite schists, chlorite-biotite schists and quarzites. These metamorphic rocks, of pre-cretaceous age, are intruded by small stocks and locally by swarms of dikes and sills.

Above these metamorphic rocks are Cretaceous volcanic and sedimentary rocks which are composed mostly of spilite, cherts and graywackes. The spilite, cherts and graywackes were highly fractured due to upthrusting of serpentinized ultrabasic rocks. The serpentinized rocks were intruded by granodiorite stock during the early stage of diastrophic activity.

Argillaceous and calcareous clastics and volcanic wackes with subordinate amount of limestones and conglomerates overlie unconformably the older rocks. This formation is well exposed southwest of San Jose Panganiban town, is of Eocene age. Folds and fault patterns exhibited are primarily due to intrusion of the granodiorite stock. The formation were uplifted and tilted to the southwest.

Volcanic materials consisting predominantly of andesite flows and tuff breccias, of probable Oligocene age were deposited above the Eocene sediments. The volcanic rocks were also tilted to a lesser degree and faults were developed.

During early Miocene time, extensive areas were covered by fine carbonaceous clastics. The Middle Miocene was a period of extensive orogeny characterized by the intrusion of diorite, diorite porphyry and syenite (?). It is believed that the diorite intrusion is generally related to mineral deposition in the area (Frost, 1959).

During late Miocene time marine and terrestrial (molasse-type) sedimentation took place contemporaneously with volcanic activity. These sediments filled the low valleys of the area.

The major fault structures in the area, represented by the thrusting of the ultramafic rocks and the parallel faults to the southwest, trend northwest-southeast, parallel to the Philippine Rift Zone.

However, tensional fractures are also numerously developed during the intrusion of the granodiorite stock. These provides channels for passage of hydrothermal solutions.

III. PRINCIPLE OF INTERPRETATION

Since strength and direction of the geomagnetic field varies with the location, the geomagnetic field is expressed by a combination of declination, inclination and horizontal intensity, vertical intensity or total intensity. Declination is the angle between the magnetic and geographical meridian. Inclination is the angle between the direction of the geomagnetic field and the horizontal plane. At the magnetic pole the inclination is exactly 90^{o} and the total intensity that is the strength of the geomagnetic field is from 60,000 to 65,000 gamma, while at the magnetic equator the inclination is exactly 0^{o} and the total intensity decreases to 30,000 -40,000 gamma.

Nevertheless the distribution of the geomagnetic field is approximated by a field dur to a bar magnet, namely a doublet located at the center of the earth, substantial distribution is more complicated than the magnetic field dur to a doublet. Deviation of the geomagnetic field from an ideal doublet field is called magnetic anomaly, among which regional anomaly or crustal anomaly extends so widely as several thousands sq km, while local anomaly or surface anomaly is less extensive than the former. The latter anomaly is useful for mineral exploration and caused by the difference in magnetic properties of rocks, that is, the anomaly is observed near the boundary between strongly and weakly magnetized rocks. Accordingly, distribution of rocks can be revealed by detecting and analyzing magnetic anomalies.

Magnetism of rocks is controled by that of the component minerals. Magnetite is the most magnetic, whereas ilmenite, pyrotite, hematite and ulvospinel are also magnetic, but their susceptibility is smaller. Other minerals are practically non-magnetic. In general, igneous and metamorphic rocks contain more magnetic than sedimentary rocks and thus much more magnetic. Although sediments filling a basin are assumed to be non-magnetic, the basement composed of various igneous and metamorphic rocks are magnetically heterogenious and thus causes various magnetic anomalies due to the boundaries of compartments separated by the differences in the magnetic properties. Subsequently, distribution of the depths of basement bordering a sedimentary basin can be obtained by interpreting magnetic

anomalies which are likely derived from these compartments. Furthermore, the distribution of compartments may correspond to the structure in the basement.

This is the principle of the application of aeromagnetic survey to the study of structure of sedimentary basin. If an intrusion of igneous rock is a compartment of the basement and in addition, the top of the intrusion is as deep as the unconformity between the sediments and the basement, the depth of magnetic anomaly indicates the depth of unconformity, or the magnetic basement agree with the geologic basement. However, in the case that intrusions did not reach up to the surface of the basement, the magnetic basement is deeper than the geologic basement.

Igneous intrusions occur also in overlying sediments. In this case, the depth of the estimated magnetic bodies is independent of the depth of the geologic basement. Since such shallow intrusions are usually small, these bodies bring on so narrow anomalies of large amplitude that the patterns are different with those of the anomalies dur to intrusive bodies within the basement.

Therefore, intrusions in the sediments can be discriminated from those within the basement by patterns of the anomalies. The top of shallower anomalies may be linearly arranged in one or several rows instead of composing a curved surface. The rows of anomalies may then represent tectonic trend. The igneous sills in the sediments also yield narrow and small anomalies and can be distinguished from the anomalies due to compartments within the basement.

If the whole basement is more magnetic than the sediments, magnetic anomalies are also derived from unduration of the unconformity. Such anomalies are of smaller amplitude and of larger wave length than those due to igneous sills.

Patterns of magnetic anomaly depend not only on magnetization, type and depth of magnetic body but also on average total intensity, inclination of the geomagnetic field in the area as well as on orientation of the magnetic body. Fig.2 shows examples of the magnetic anomalies due to a magnetic prism in five orientations in the case that inclination is 15^{o}N. These figures represent change of pattern

with the orientation, whereas positive parts of the anomalies appear always to the south of the prism and negative to the north.

In the case of the examples illustrated in Fig.2, magnetization is caused by induced magnetization due to the current geomagnetic field. Interpretation of magnetic anomalies is ordinarily made by assuming that induced magnetization is the main origin of magnetic anomalies. However, magnetic anomalies are generated also by remnant magnetization. Besides, magnetic substance has a certain degree of remnant magnetism. Strength and direction of remnant magnetization is particular to materials, being independent of the strength and direction of the current geomagnetic field. Patterns of magnetic anomalies are sometimes influenced remarkablely by remnant magnetization, particularly when the direction of the remnant magnetization deviates from the direction of the geomagnetic field. Remnant magnetization can be measured by samples taken from rocks, however it is impossible to collect rock samples of the basement overlain by thick sediments especially in case of reconnaissance surveys.

Direction and strength of remnant magnetization, as well as magnetic susceptibility are not always homogenous throughout a compartment of basement. Only average formation magnetization is reflected in magnetic anomalies recorded by the aeromagnetic survey. Induced magnetization coincides with the geomagnetic field in direction, while direction of remnant magnetization is normally at random. Total magnetization of a magnetic rock body may thus be reduced and average formation magnetization is mainly contributed by average induced magnetization. Interpretation of aeromagnetic survey data is usually made by taking only average susceptibility in consideration.

It should be noted that remnant magnetization of shallow intrusion mitht have to be considered because comparatively small intrusion of volcanic rocks is occasionally characterized by homogenous remnant magnetization and may disturb the determination of magnetic basement.

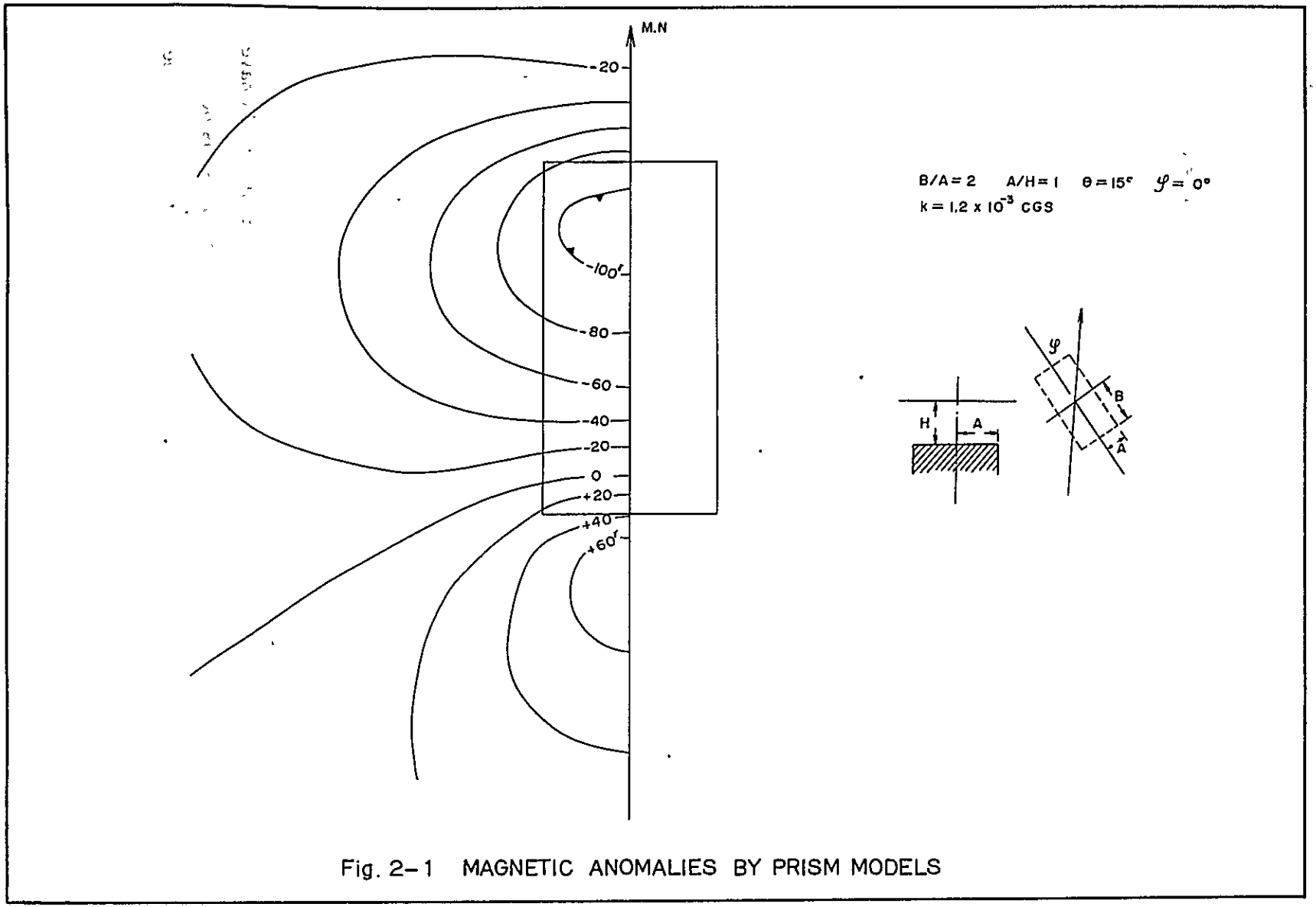

Fig. 2-1 MAGNETIC ANOMALIES BY PRISM MODELS

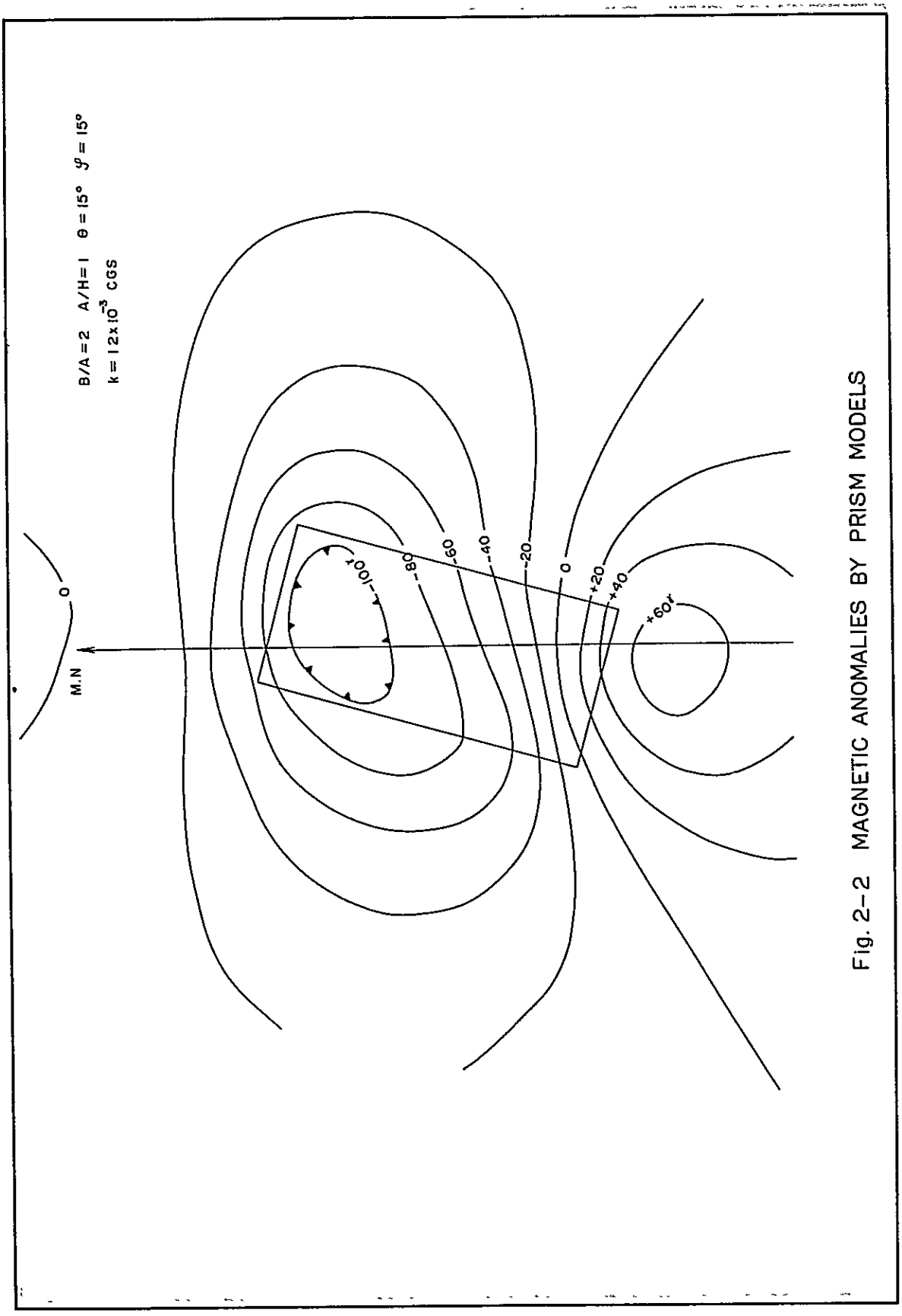

Fig. 2-2 MAGNETIC ANOMALIES BY PRISM MODELS

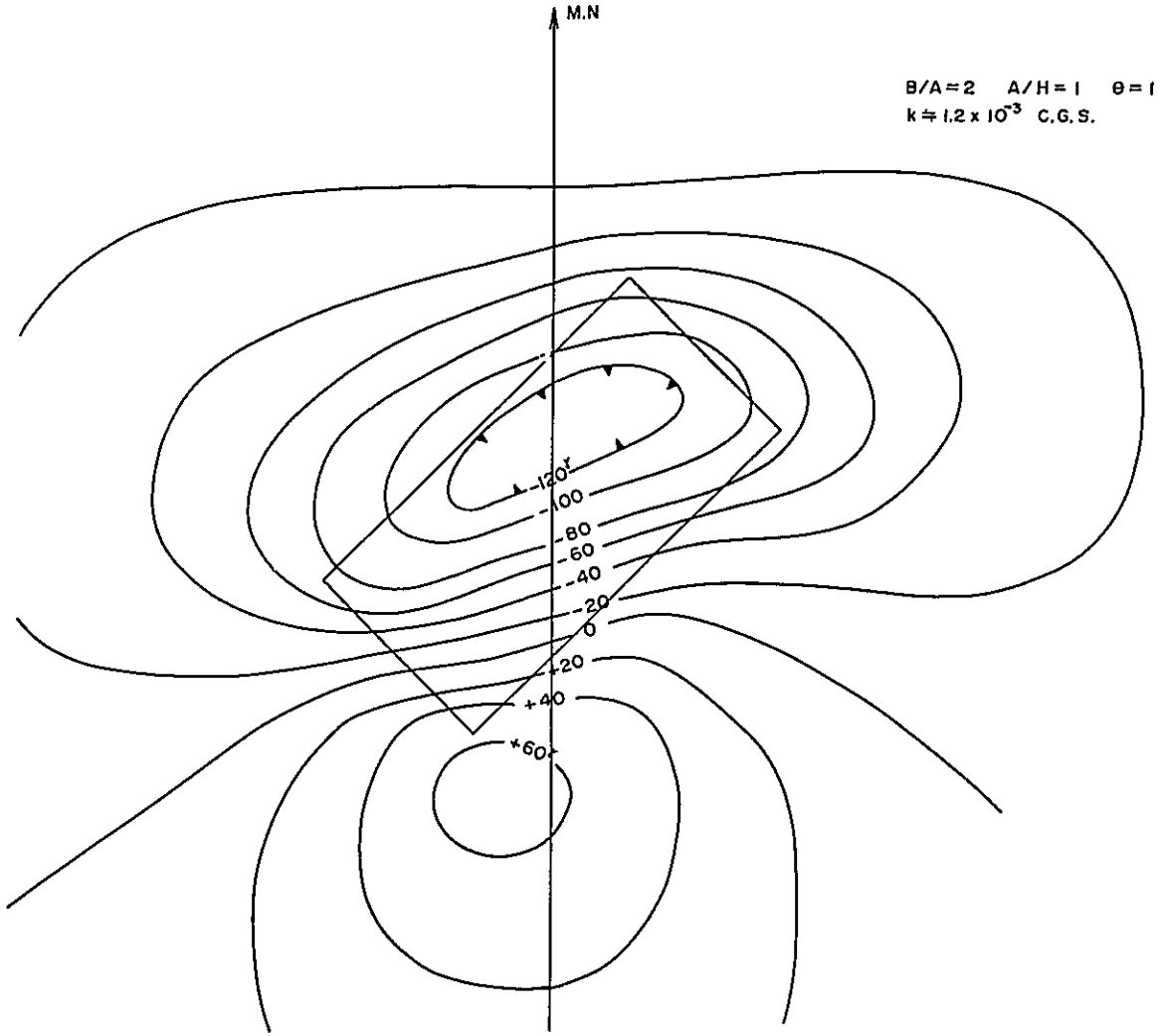

Fig. 2-3 MAGNETIC ANOMALIES BY PRISM MODELS

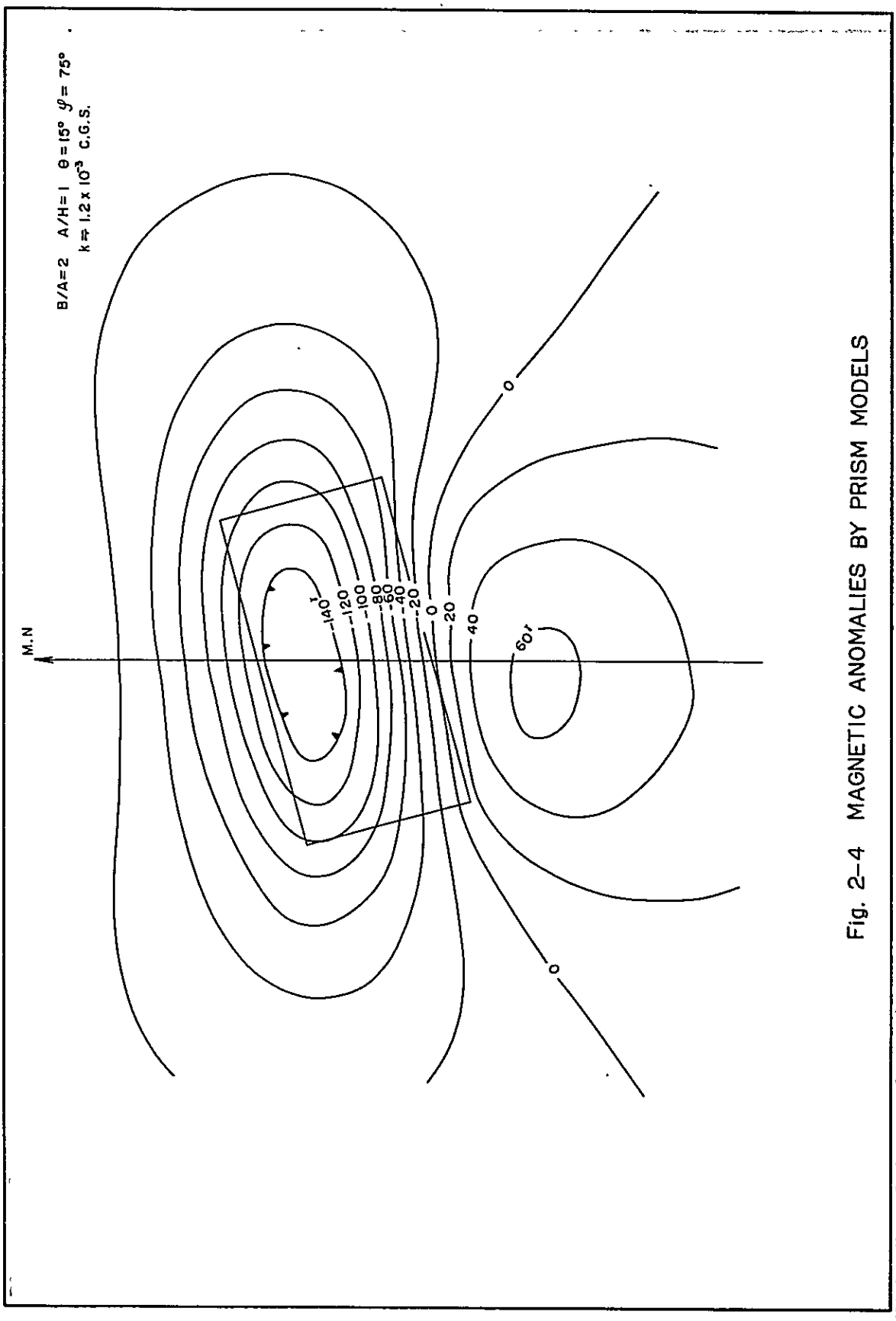

Fig. 2-4 MAGNETIC ANOMALIES BY PRISM MODELS

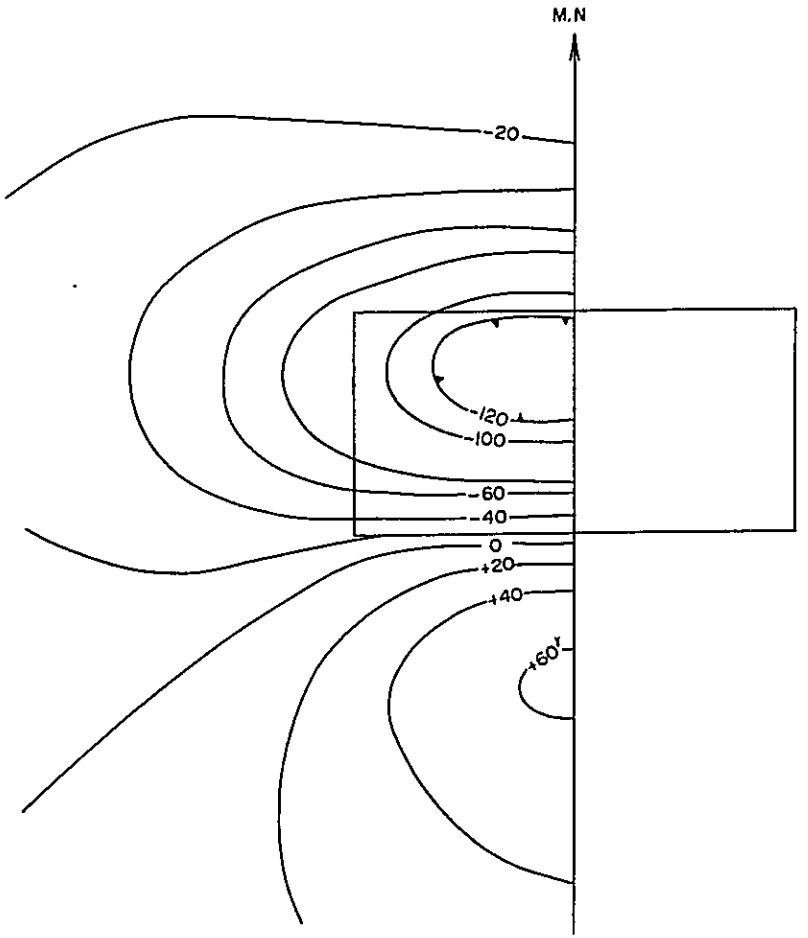

A/B = 2 H/A = 1 θ = 15° φ = 90°

k = 1.2 x 10^{-3} C.G.S.

Fig. 2-5 MAGNETIC ANOMALIES BY PRISM MODELS

IV. METHOD OF INTERPRETATION

It is necessary to presume the type of subsurface structure from the pattern of magnetic anomaly before undertaking quantitative interpretation. In qualitative interpretation, preliminary concepts of geology should be built up by presumption of such subsurface structures as distribution of fractures or lithologic changes in the basement, or intrusions in the sediments. Then, depth and susceptibility of magnetic body can be calculated based on the concept obtained by qualitative interpretation. Magnetic basement map can be finally drawn up.

Total magnetic intensity ΔT and its second derivative $\frac{\partial^2 T}{\partial Z^2}$ of two-dimensional magnetic body are expressed by comparatively simple mathematical equations of linear combination of even and odd functions.

$$\Delta T = 2KTA^2 \sin\delta \left\{\cos 2I_0' \times \phi_x + \sin 2I_0' \times \lambda_x\right\} \quad (1)$$

$$\frac{\partial^2 T}{\partial Z^2} = 2KTA^2 \sin\delta \left\{\cos 2I_0' \times \partial^2\phi_x / \partial Z^2 + \sin 2I_0' \times \partial^2\lambda_x / \partial Z^2\right\}. \quad (2)$$

where K: susceptibility,

T: total intensity of the geomagnetic field,

A: intensity attenuation factor, namely, A = sinI/sinI',

I : inclination of the geomagnetic field,

I': effective inclination, namely, $I' = \tan^{-1}(\tan I/\tan\delta)$,

I_0': $I' + \frac{\pi}{4} - \frac{d}{2}$.

In addition, δ is the angle between the magnetic north and the trend of magnetic body or fault; and d is the dip of magnetic body or fault to horizontal plane.

ϕ_x is a function determined by the angle between two lines connecting the edge of a magnetic body and is an even function for dyke model and an odd function for step model. λ_x is a logarithmic function determined by logarithm of ratios of the distances between observation point and the edges of a magnetic body. It is an odd function for dyke model and an even function for step model.

Fig.3 shows the relations between φ and I' and between φ and A^2 in the case that inclination is 15^{o}N that is the average value in the surveyed area. A^2 deoreases rapidly with the decrease in φ from the value of $A^2 = 1$ when $\varphi = 90^{o}$ and becomes 1/5 when $\varphi = 25^{o}$. Therefore, total magnetic anomaly decreases with φ. On the contrary, I' increases with the decrease of φ from the value of $I' = +15^{o}$ when $\varphi = 90^{o}$ and reaches to $+45^{o}$ approximately when $\varphi = 18^{o}$.

On the other hand, the function $\{ \cos 2I_0' \times \emptyset_x + \sin 2I_0' \times \lambda_x \}$ for dyke model varies with I_0' as shown in Fig.4 and is equivalent to $\emptyset_x$ and λ_x respectively when $I_0' = 0^{o}$ and $I_0' = 45^{o}$. Therefore, negative part of anomaly predominates when $I_0' = 0$ and it attenuates gradually as I_0' tends to 45^{o}. Then, negative part of anomaly is equal to positive part when $I_0' = +45^{o}$. Subsequently, negative part of anomaly decreases with the decrease of φ from 90^{o}. This is quite similar to the changes of pattern of anomaly due to prism model, in which negative part located to the south of the center of the prism recedes from the center as decreases and the amplitude of negative anomaly decreases also with the decrease of

As shown above, patterns of total intensity anomaly remarkablely change with deviation of the strike and dip d of magnetic body. The result is also valid for the second derivative because the equation (2) is similar to (1). Fig.5 and Fig.6 show profiles of the total magnetic intensity and the second vertical derivative, calculated from (1) and (2) respectively, in the case that the ratio of the half-width a of magnetic body to the depth h, a/h is 0.2, 0.5, 1.0, 1.5 and 2.0, assuming T = 40,000 gamma and $K = 1.19 \times 10^{-8}$ C.G.S..

It may be seen from the figures that magnetic anomaly becomes greater as width of magnetic body becomes broader, if the top of the body remains constant, and horizontal attenuation of anomaly is also effected. In contrast, amplitude as well as horizontal attenuation of anomaly becomes smaller as the top of magnetic body become deeper, if the width of the body is unchanged. Various methods for determination of the depth are based on such fact that amplitude of anomaly decreases and its wave length increases as the top of magnetic body becomes deeper. Another

characteristic is that gradient of anomaly curves is nearly the maximum at the boundaries of magnetic body, in other words, the second vertical derivative tends to zero approximately at the boundaries. The distance between inflection points of second derivative is about 2a if a/h = 1. If a/h$\underline{1}$1, the distance is larger than 2a and equal to about 1.3 h when a/h = 0.2. The distance is controled by the depth of the top of magnetic body when a/h is greater than 1. It can be pointed out from Fig.5 and 6 that the length of straight portion of both the total intensity and the second derivative curves is nearly constant independently of width of magnetic body.

Fig.7 and 8 illustrate the total magnetic intensity and the second derivative due to "Graben" structure calculated by step model, assuming that inclination is $+15^{o}$ and total intensity is 40,000 gamma. The calculation was conducted in the case that the ratio of throw 1 to the depth h, 1/h is 0.2 and the ratio of the width W of "Graben" to the depth, 2W/h is 2.0, 1.0, 0.5 and 0.25. Swell of the basement corresponds to significantly negative part of anomaly, while graben or depression corresponds to positive part and inflection point appears at the edge like dyke model. Similarly, the distance between inflection points is approximately equal to 2W if W/h = 1 and it becomes longer than 2W if W/h 1. The distance is equal to h when W/h is about 0.125.

As mentioned above, the inflection points of total intensity curve may indicate the edge of a broad magnetic compartment whose width is greater than the depth of top.

Isolated magnetic anomaly due to a magnetic body is occasionally influenced by the effect of adjacent magnetic bodies and total intensity and second derivative curves are thus distorted. Sometimes, even several neighbouring magnetic bodies yield single magnetic anomaly. Fig.9 and 10 show the total intensity and the second derivative for two neighbouring magnetic bodies of which the ratio of the width to the depth is both 0.2.

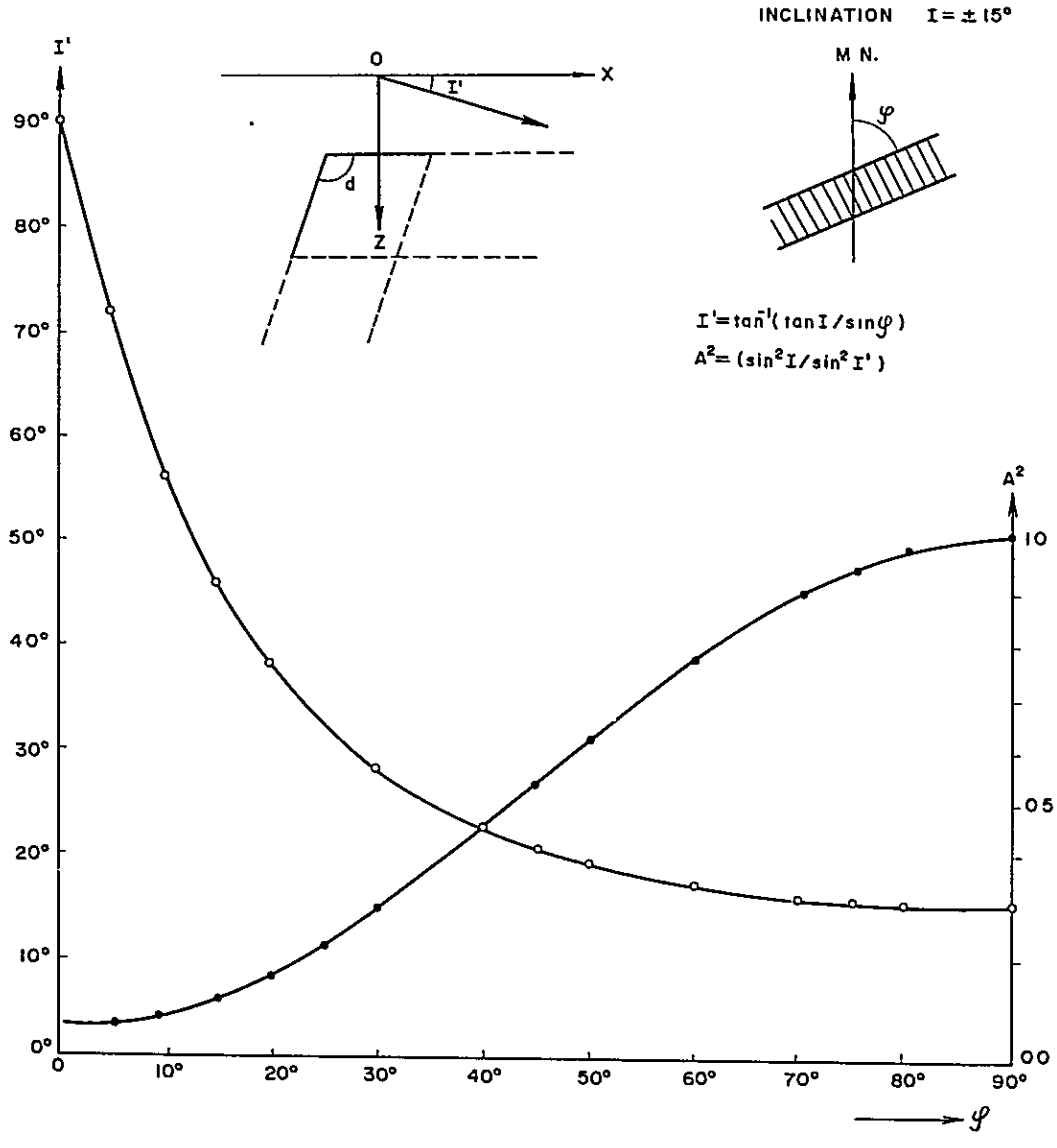

Fig. 3 $I^2-\varphi$, $A^2-\varphi$ RELATIONS

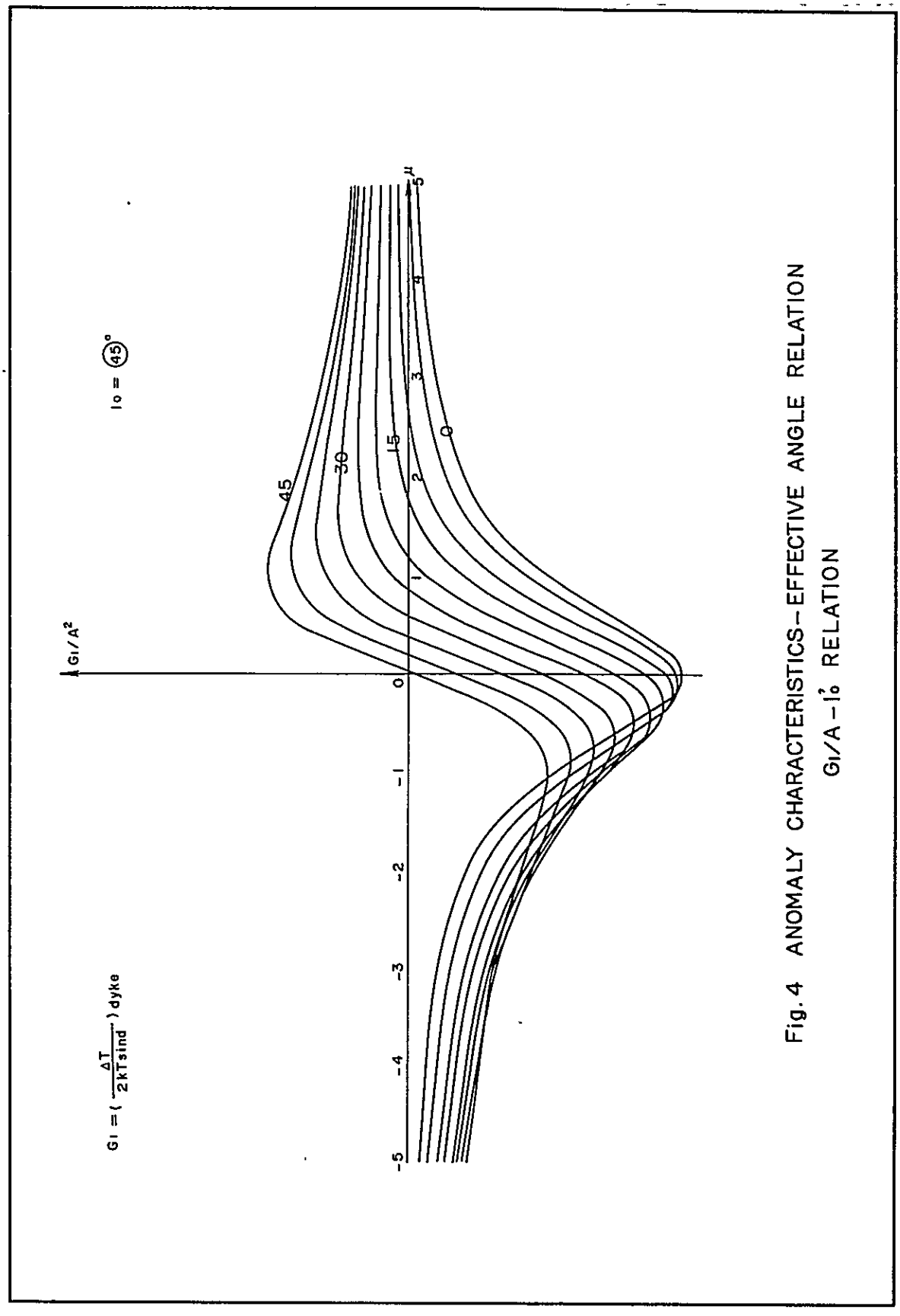

Fig. 4 ANOMALY CHARACTERISTICS–EFFECTIVE ANGLE RELATION

$G_1/A - I_0^2$ RELATION

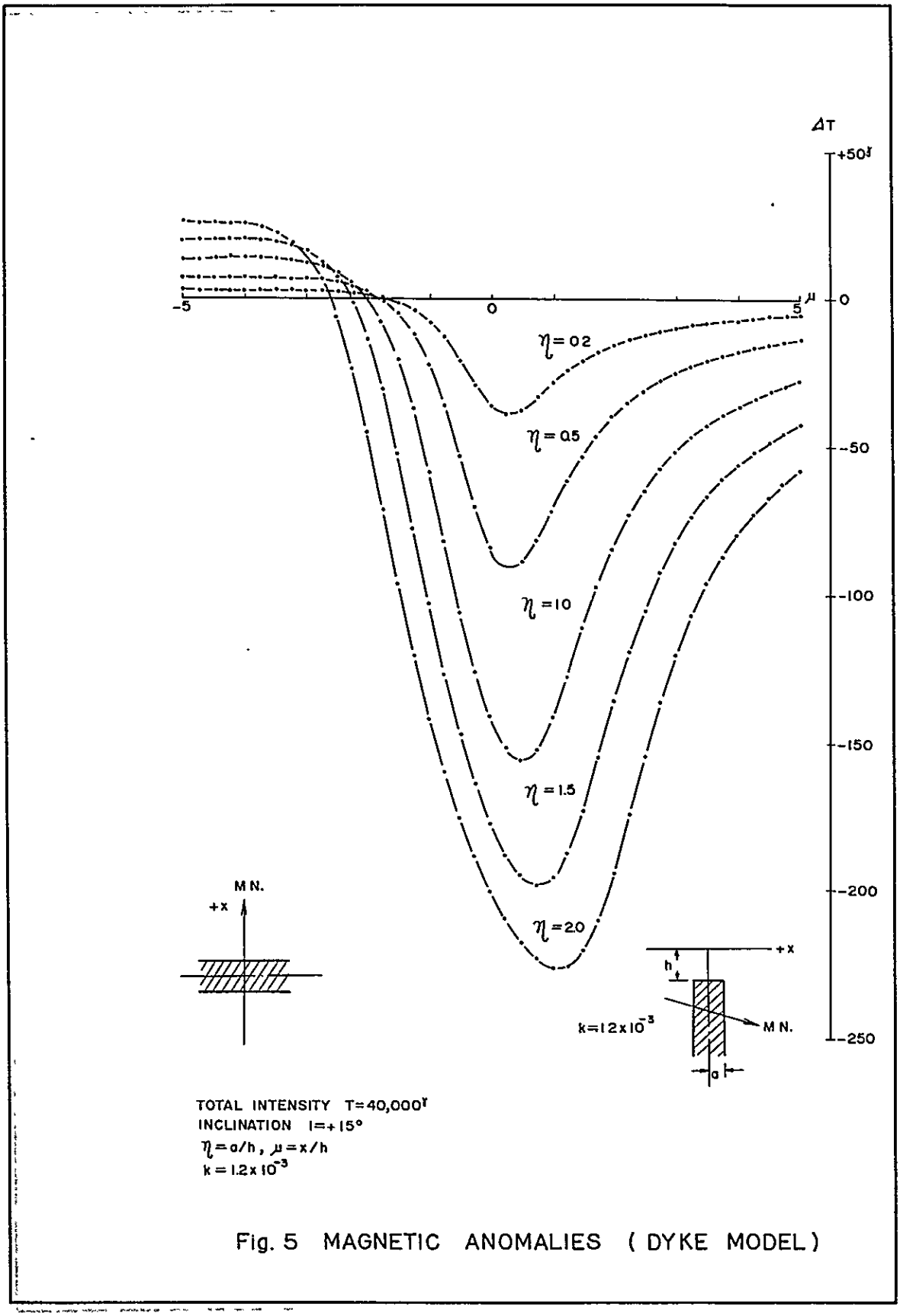

Fig. 5 MAGNETIC ANOMALIES (DYKE MODEL)

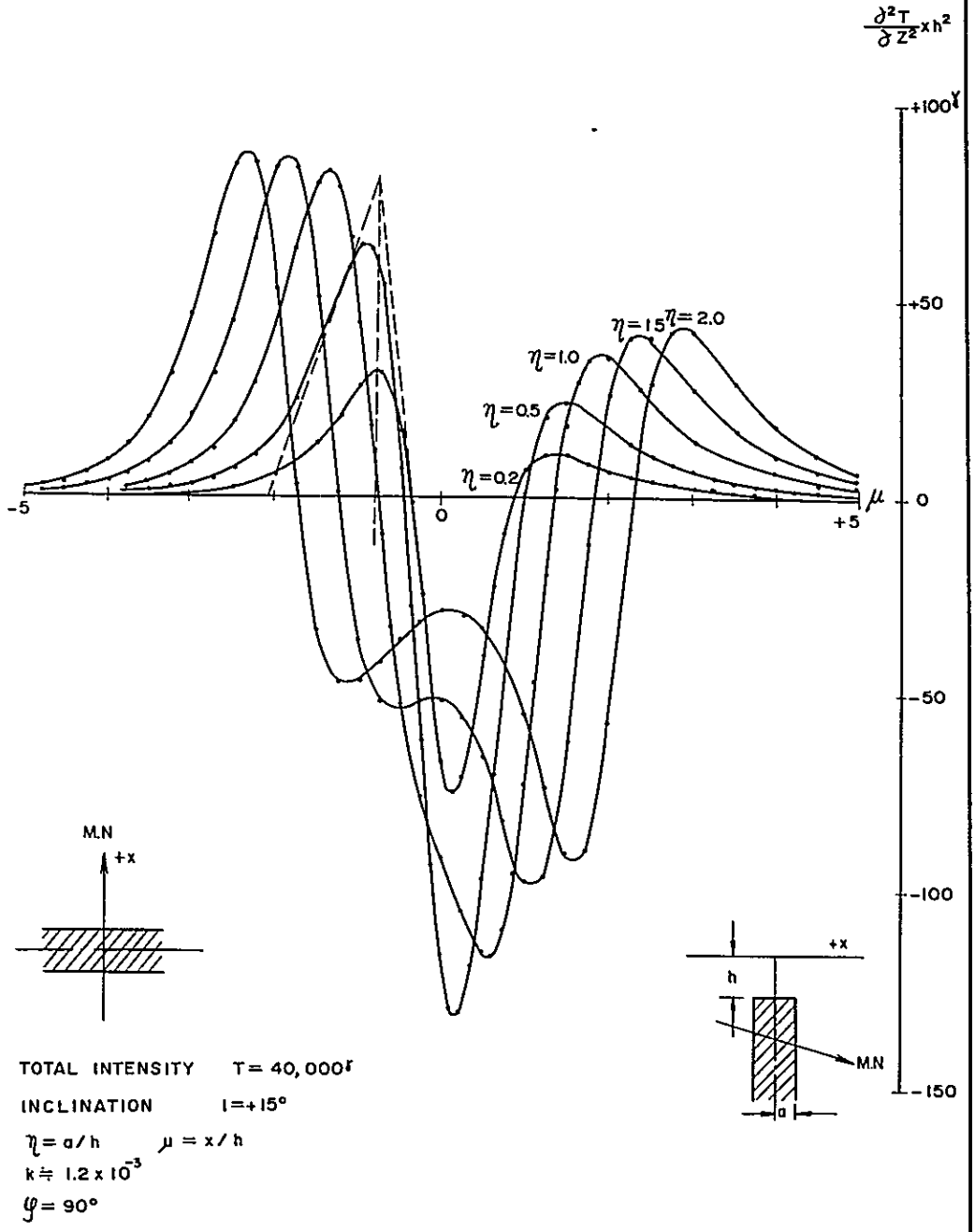

Fig. 6 SECOND VERTICAL DERIVATIVE ANOMALIES (DYKE MODEL)

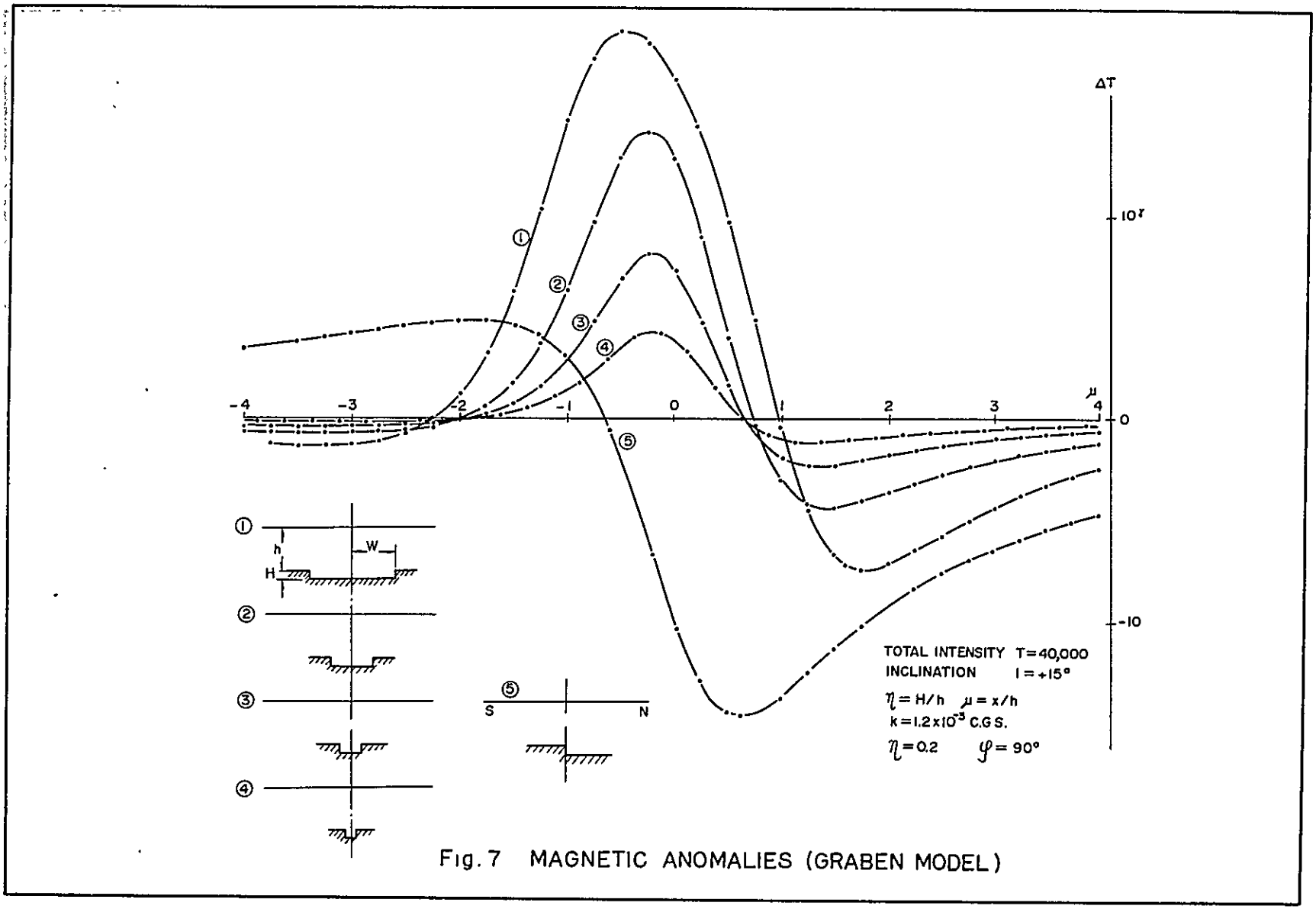

Fig. 7 MAGNETIC ANOMALIES (GRABEN MODEL)

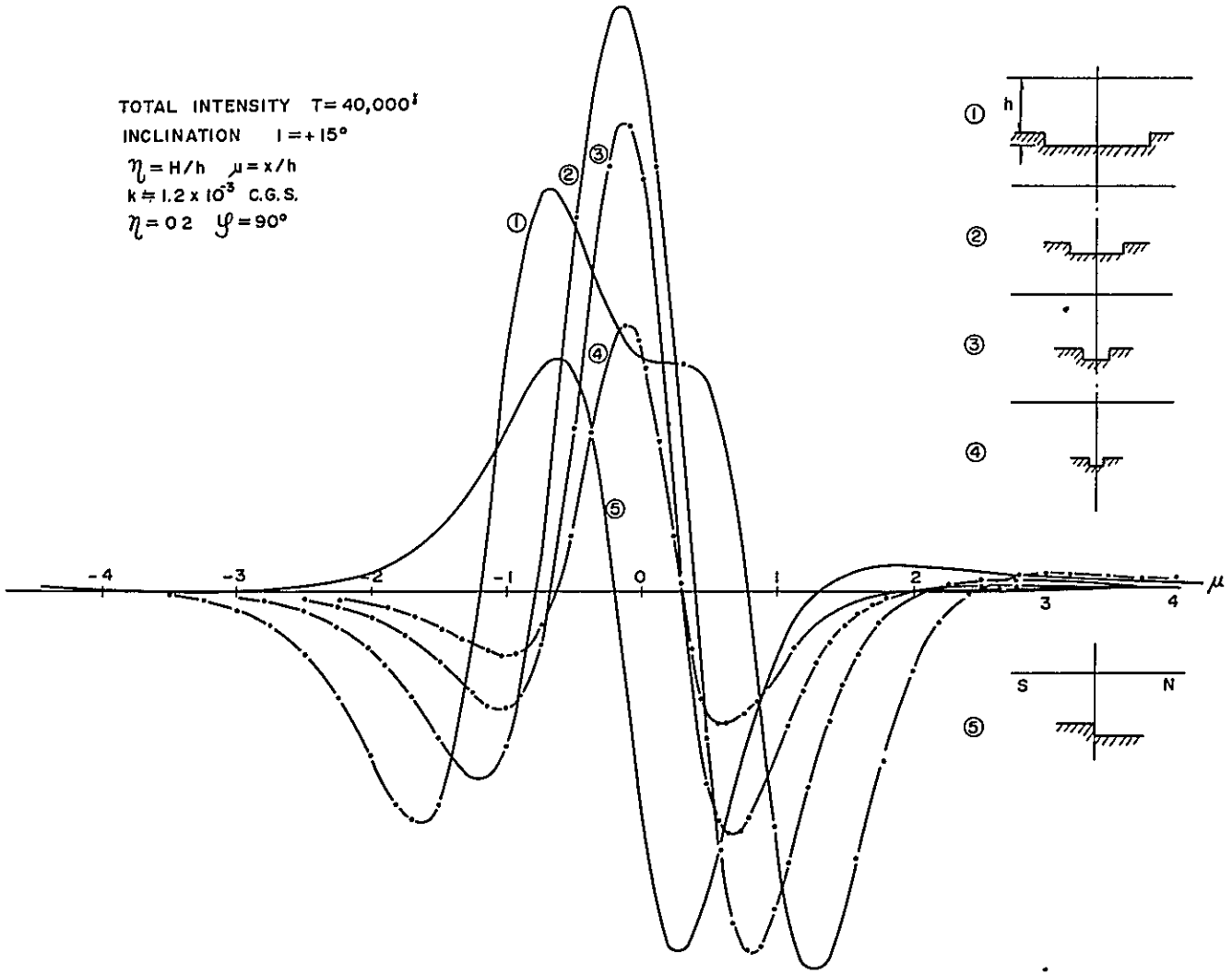

Fig. 8 SECOND VERTICAL DERIVATIVE ANOMALIES (GRABEN MODEL)

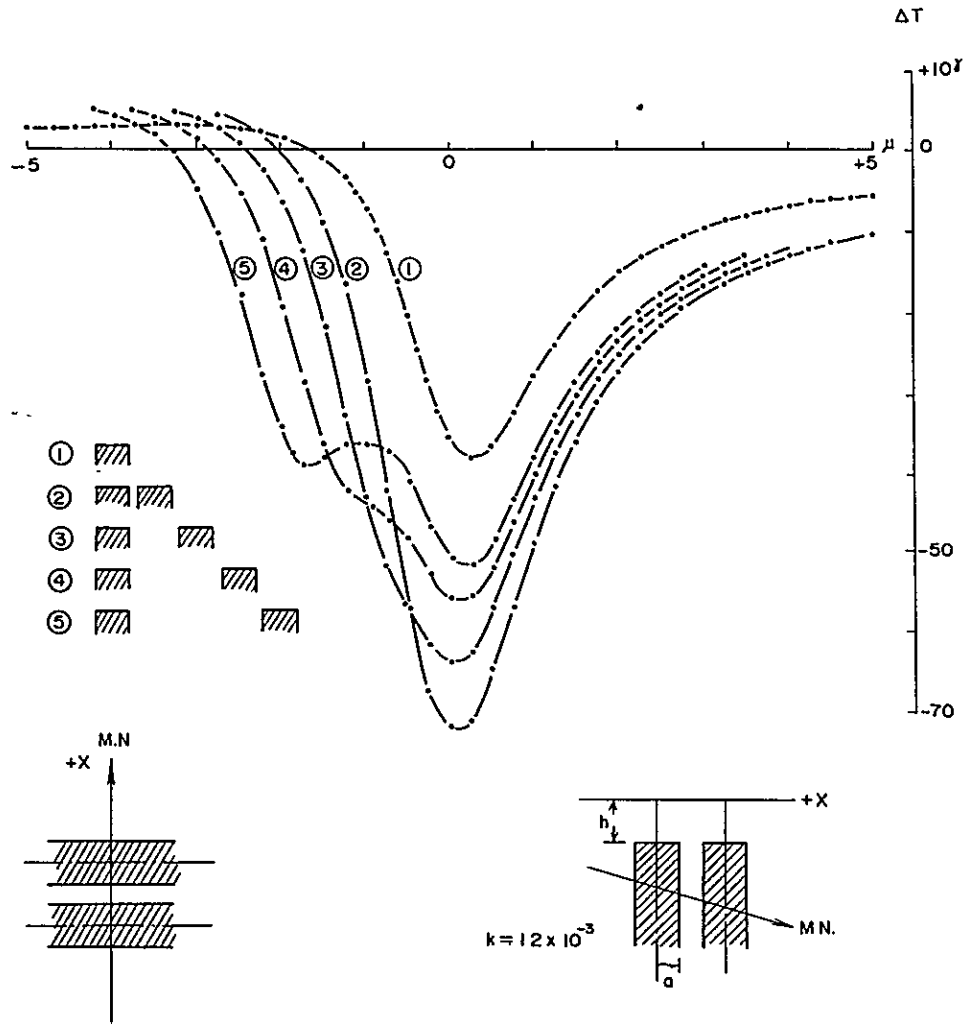

TOTAL INTENSITY T=40,000γ
INCLINATION I=+15°
$\eta = a/h \quad \mu = x/h$
$k = 12 \times 10^{-3}$
$\eta = 90° \quad \varphi = 0.2$

Fig. 9 MAGNETIC ANOMALIES (DYKE MODEL)

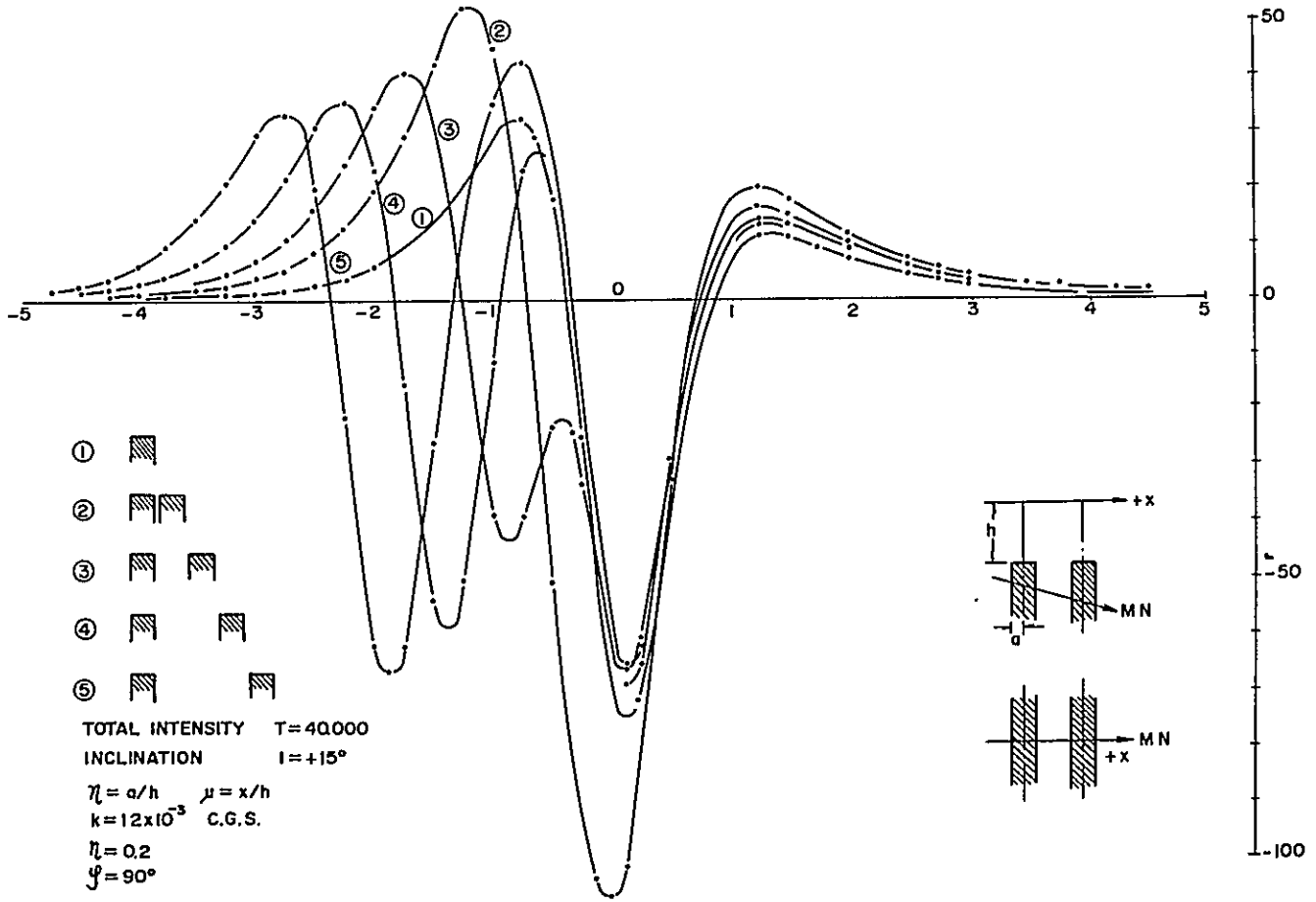

Fig. 10 SECOND VERTICAL DERIVATIVE ANOMALIES (DYKE MODEL)

The distance S between the centers of two magnetic bodies is 1.25 x 2a, 2.5 x 2a, 3.75 x 2a and 5 x 2a. As shown in Fig.9 and 10, although the total intensity due to deeper magnetic bodies is practically regarded as single anomaly when S/h is less than 1.5, the two bodies can be completely resolved by investigating second derivative even S/h = 1.5. Second vertical derivative is better in resolving neighbouring bodies. However, to differentiate the effect of two adjacent magnetic bodies is impossible when S/h is less than 0.75 and quantitative interpretation may be very difficult even when S/h = 1. In such case quantitative interpretation needs a certain assumption and several solutions may be possible.

As hitherto mentioned, pattern of anomaly is influenced by several parameters. In quantitative interpretation, magnetic bodies are ordinarily assumed as those of simple configulation, homogeneously magnetized and of 90^{o} in dip. Even under these assumptions, unique solution may not be obtained. Geologic concepts derived from qualitative interpretation must be taken into consideration.

Quantitative method for interpretation can be classified into three categories, the analytical method, the specific point method and the curve matching method.

An analytical method for interpretation of gravity anomaly was developed by Tsuboi and Fuchida (1937, 1938) and was later modified by Nagata (1938) in order to apply to anomalies of horizontal and vertical magnetic intensity. Recently, several methods have been proposed for the interpretation of total magnetic intensity anomaly. (Bhattacharia, 1965; Hahn, 1965; Segawa, 1967)

Observed magnetic field can be analytically represented by a double Fourier series, while horizontal distribution of magnetization can be also expressed by a double Fourier series if subsurface magnetization is condensed into a horizontal thin plate at a certain depth. The latter Fourier series can be transformed from the former Fourier series by the aid of potential theory. If the magnetization is assumed to be constant in this method of interpretation, the deviation from an average condensation depth can be represented by a double Fourier series, provided that an average

condensation depth and an average magnetization are previously given by a certain means.

Analytical methods are very useful for two-layered structure in which the whole basement homogeneously magnetized is somewhat more magenetic than the overlying sediments. These methods can determine pertinently the undulation of the basement. Another advantage of the methods is that the analytical procedures can be extensively conducted by computor, reducing mannual processing to a minimum.

However, two-layered structure is rather rare as subsurface structure model for magnetic anomalies, whereas it is generally appropriate for the interpretation of gravity anomalies. As mentioned before, magnetic anomalies over sedimentary basin area are caused by difference of magnetization of compartments in the basement or igneous bodies in the sediments, namely, by lateral change in magnetization. Accordingly, analytical methods which disregard lateral change might lead to noticeable error.

Most magnetic anomalies observed in the present survey were proved to be due to difference of magnetization in the basement or to younger igneous body in the sediments, by comparing the distribution of anomalies on land with the geology. In addition, no data are available suggesting average condensation depth and average magnetization, for instance, no deep well data are available in the surveyed area. Analytical methods were, therefore, not applied.

On the other hand, straight slope method proposed by Vacquire et al. (1963), as well as characteristic curve methods proposed by Moo (1965), Grant(1966) and Giret and Naudy (1957), belong to specific points methods, while curve matching methods were proposed by Gay (1963), Chastent and Naudy (1957). Among these mothods, only the method by Vaquier makes the use of second vertical derivative also.

Various magnetic anomaly curves due to prism, dyke and step (fault) models had been calculated by the Geological Survey of Japan. Based on these theoretical curves, depth indexs for straight solpe length and inflection tangent length were obtained assuming that average total intensity and average inclination are 40,000 gamma and $+15^{o}$ respectively in the area surveyed. The definitions of the parameters, straight slope length and inflection tangent length, are shown in Fig.11. Depths of magnetic bodies were determined by multiplying the depth index to the observed values of the parameters.

Although the definition of straight slope length is analytically ambiguous, the past experiences proved that this method gave excellent result and particularly when the application of depth indexs is considered together with other informations on depths of magnetic bodies and empirical correction for particular area is combined, accurate determination of depths can be expected. In the present interpretation, the method using inflection tangent length was also employed as an auxiriary means.

In conducting this procedure, reproducibility of the parameters was carefully examined by comparing three adjacent profiles and the observed pattern was carefully compared with the calculated pattern of model so that the error due to distortion of pattern by interference with adjacent anomaly was reduced to a minimum. By this procedure, determination of depths of many magnetic anomalies could be carried out during comparatively short time. Actually, depth determinations for 239 sections was made.

After the determination of depths and types, apparent magnetic susceptibility was estimated by comparing the observed anomaly with computed one. Concurrently, the coincidence between the observed and calculated patterns was investigated by curve matching method. In the case of anomalies interfered remarkablely with adjacent ones, the type and depth of northernmost (or southernmost) magnetic body were roughly estimated at first and then, the calculated anomaly for the estimated magnetic body was subtracted from the observed anomaly. The residual anomaly was treated successively for further estimation. The trial and error method was

conducted by using an average susceptibility obtained from the neighbouring anomalies and by taking into consideration the structural and geologic concepts from previous qualitative interpretation.

(A) MAGNETIC ANOMALY

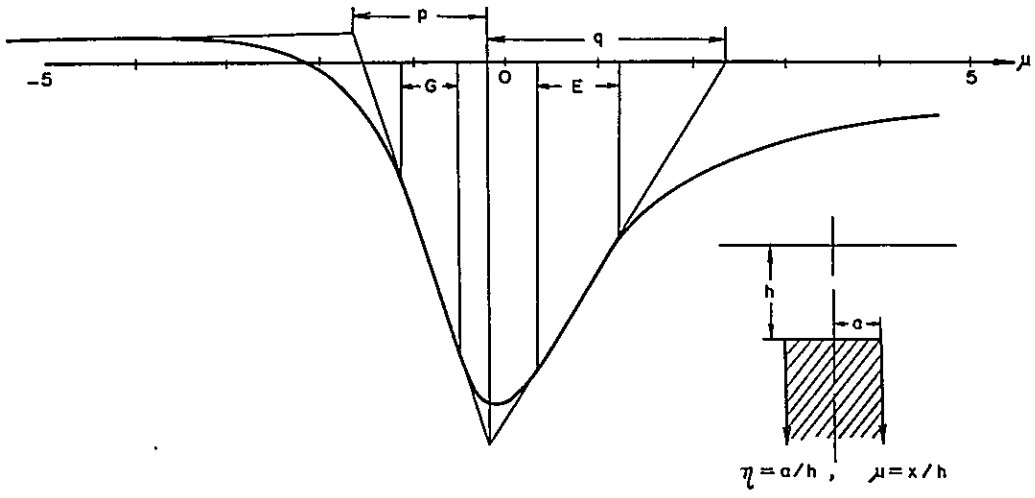

(B) SECOND VERTICAL DERIVATIVE

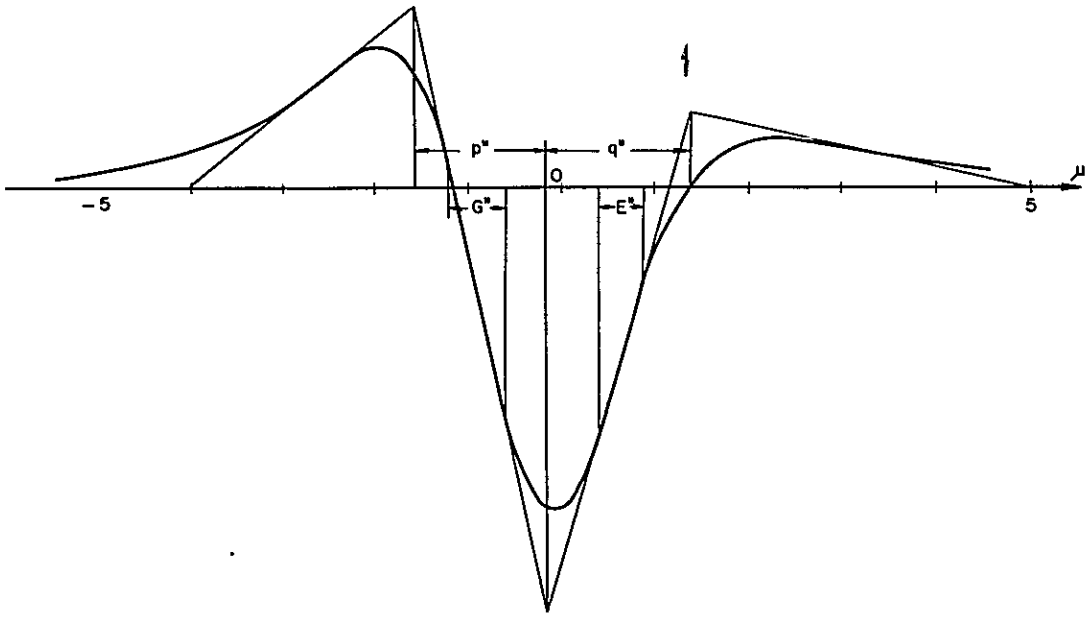

INFLECTION TANGENT LENGTH : P . q . p" . q"
STRAIGHT SLOPE LENGTH : G . E G" . E"

Fig.11 INFLECTION TANGENT LENGTH & STRAIGHT SLOPE LENGTH

V. EQUIPMENT AND SURVEY PROCEDURES

V-1. Airborne magnetometer

Varian Model V 4914 airborne magnetometer which was used for the present survey measures the strength of geomagnetic field based on Larmor precession by magnetic spin characteristic of proton. Proton exhibits precession around geomagnetic field like a rotating bar magnet and its precessional frequency f_p is proportional to the strength of the geomagnetic field; hence,

$$T = 23.4868 \times f_p,$$

where T is the strength of the geomagnetic field expressed in gauss and f_p is expressed in Hz unit.

Average magnetization of protons in hydrocarbon solution is oriented in the same direction as the geomagnetic field in their normal state, however only small portion of protons are arranged in parallel to that direction. The signal derived from the precession is, therefore, undetected. If magnetic field of about two hundreds times as strong as the geomagnetic field is applied perpendicualrly to the geomagnetic the geomagnetic field is applied perpendicularly to the geomagnetic field, large portion of protons in a solution will be lined up in the direction of the applied magnetic field. Then, if the applied field disappears suddenly, majority of protons arranged in a given direction will commence the precession at the same phase. In this case, signal enough for detection can be generated.

The sensor contains a container of hydrocarbon solution (kerosene or a mixture of kerosene and motor oil) inserted into a coil placed in the direction perpendicular to the geomagnetic field. An electric current is sent to the coil so that a magnetic field of about two hundreds times as strong as the geomagnetic field can be induced. Then, if the current is turned off, signal voltage will be generated in the coil by the precession of protons. Since the frequency of the voltage is proportional to the strength of the geomagnetic field and the factor is characteristic of proton, the

measurement of frequency of the signal geves the strength of the geomagnetic field.

Fig. 12 illustrates the block diagram of the airborne magnetometer. Sensing coil is connected with precession signal counting circuit after excitation, through automatic tuning and amplifying circuit. Precession frequency is measured by the following precession frequency counter which contains a reference oscillator of 400 kHz by which the gate of the main circuit is controled.

The analog recorder is driven by analog output of the D-A converter and displays the frequency measured by the precession frequency counter. Feducial and time marks are also recorded on the analog magnetic record by the signals from an aerial camera and a standard clock so that magnetic record can be correlated with the corresponding position of track chart.

Sensing head of proton magnetometer is not necessary to be kept in a definite direction, while the sensitivity depends upon the geomagnetic field. If strength of the geomagnetic field is 41615.59 gamma, the precession frequency is 1771.872 Hz. Accordingly, the sensitivity is 0.36 gamma if the gate time cycle of the precession signal counting circuit is set at 512 Hz.

V-2. Station magnetometer

Varian Model V 4938 G Cesium or Rubidium magnetometer was used for observation of time variation and magnetic storm. By the observation the quality of the records of airborne magnetometer was evaluated and the diurnal variation of the geomagnetic field was eliminated.

The cesium or rubidium magnetometer is based on the phenomenon of optical pumping and monitoring. Single valence electron of Alkaline vapour atoms like cesium or rubidium have several energy levels which are separated into several sub-levels due to Zeeman effect. The separation of sub-levels is controled by the strength of external magnetic field. In the case of cesium 133 vapour, the separation

is 3.497 Hz per gamma. Therefore, a self-exciting atomic oscillator which continuously generates Larmor frequency can be constructed by applying the technique of optical pumping and monitoring. The Larmor frequency indicates continuously the geomagnetic field. Because the Larmor frequency of cesium 133 is about one hundred times as high as that of proton, the measurement of the geomagnetic field also become sensitive by the same factor.

Fig.13 shows the block diagram of the rubidium magnetometer. Larmor frequency of the atomic oscillator (self oscillator) consisting of sensor and sensor electrohics is measured directly by a counter and simultaneously mixed with a frequency of the local oscillator. The mixed frequency is fed to the saturable magnetic core type frequency discriminator which put out direct current voltage proportional to the frequency. The analog recorder is driven by this direct current voltage and displays continuously the strength of the geomagnetic field. Absolute values of the strength of the geomagnetic field obtained by the measurement of Larmor frequency are also recorded every thirty minutes together with time marks every one minute.

In the present survey, the geomagnetic field was continuously observed with an accuracy of 0.1 gamma and the observational results were used for reducing the records of airborne magnetometer to a reference magnetic level.

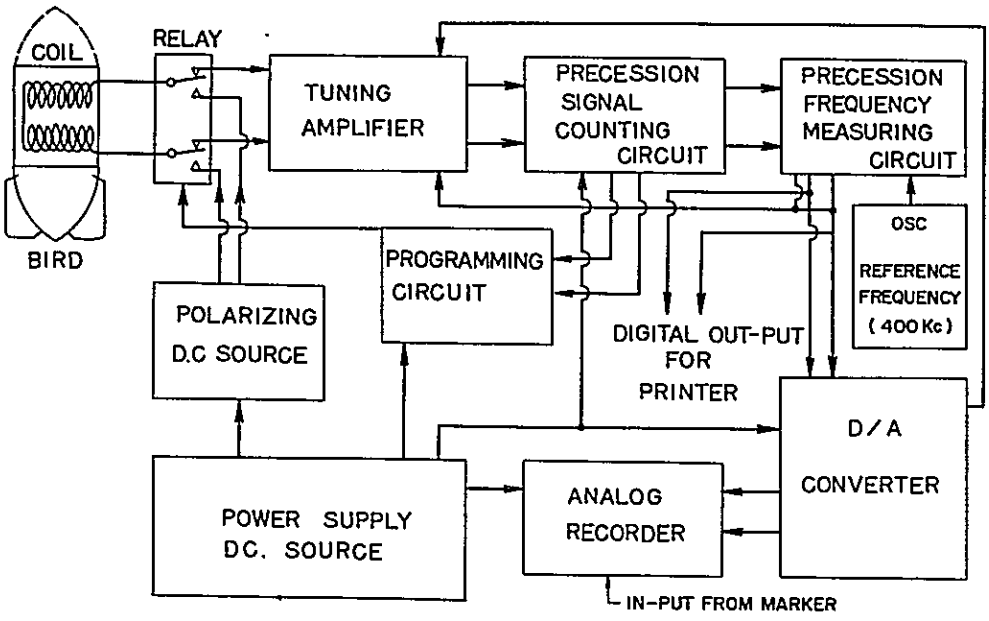

Fig.12 BLOCK DIAGRAM OF MAGNETOMETER (PROTON)

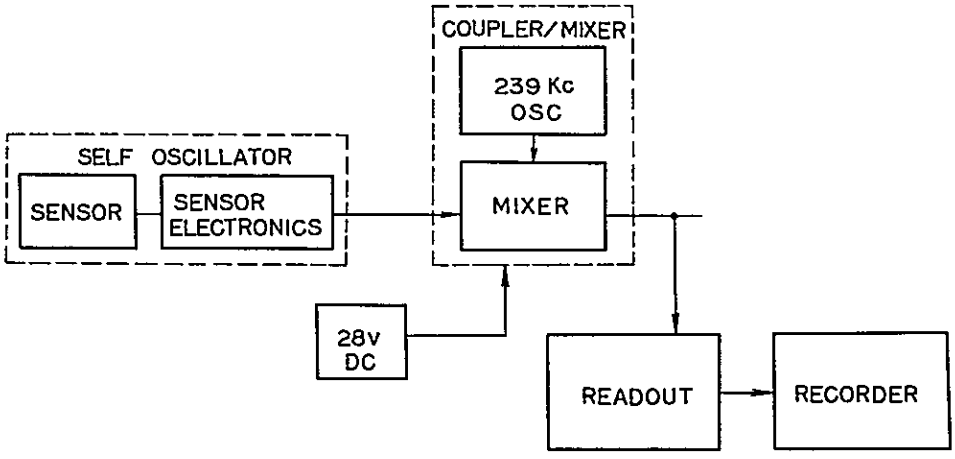

Fig.13 BLOCK DIAGRAM OF RUBIDIUM MAGNETOMETER

V-3. Navigation system

Loran-A was used as navigation system in the present survey; the equipment was Furuno Electric Model LR-2A receivers for aircraft. Loran-A is a radio navigation system useful for offshore operation, based on the fact that propagation velocity of electric wave is constant.

Synclonized Loran-A pulses borne by the carriers of a fixed frequency are transmitted from a couple of stations consisting of Master station and Slave station. Loran-A receiver on an aircraft receives the electric waves and measures the time difference between the pulse waves from a couple of the stations. A locus of the points of equal time difference is a hyperbola and is called a line of position. If various lines of position given by a definite couple of stations are laid down on a map, a line of position corresponding to instantaneous position of aircraft can be easily determined. If another line of position on which the aircraft is located is determined by similar procedure based on another couple of transmission stations, the instantaneous position of the aircraft can be determined as the cross point of the two lines of position. Fig.14 shows the notations given to the couples of the Loran-A transmission stations utilized for the present survey and the representative lines of position.

Navigation, that is, pilotage of aircraft along a predetermined track, is commonly conducted by Doppler navigation system in the aeromagnetic survey by the Geological Survey of Japan. Because Doppler system was not available for this particular survey due to unavoidable reasons, Loran-A system was employed not only for position determination but also for navigation. Subsequently, the navigation was not easy and the flight paths were frequently forced to deviate from predetermined tracks.

Before the undertaking of the survey flights, the traverses had been planned to be parallel with lines of position belonging to a couple 2H3 so that navigation would be conducted by maintaining constant time difference of Loran-A pulses. The other couple 1L6 was selected for combination if the position determination. However, it

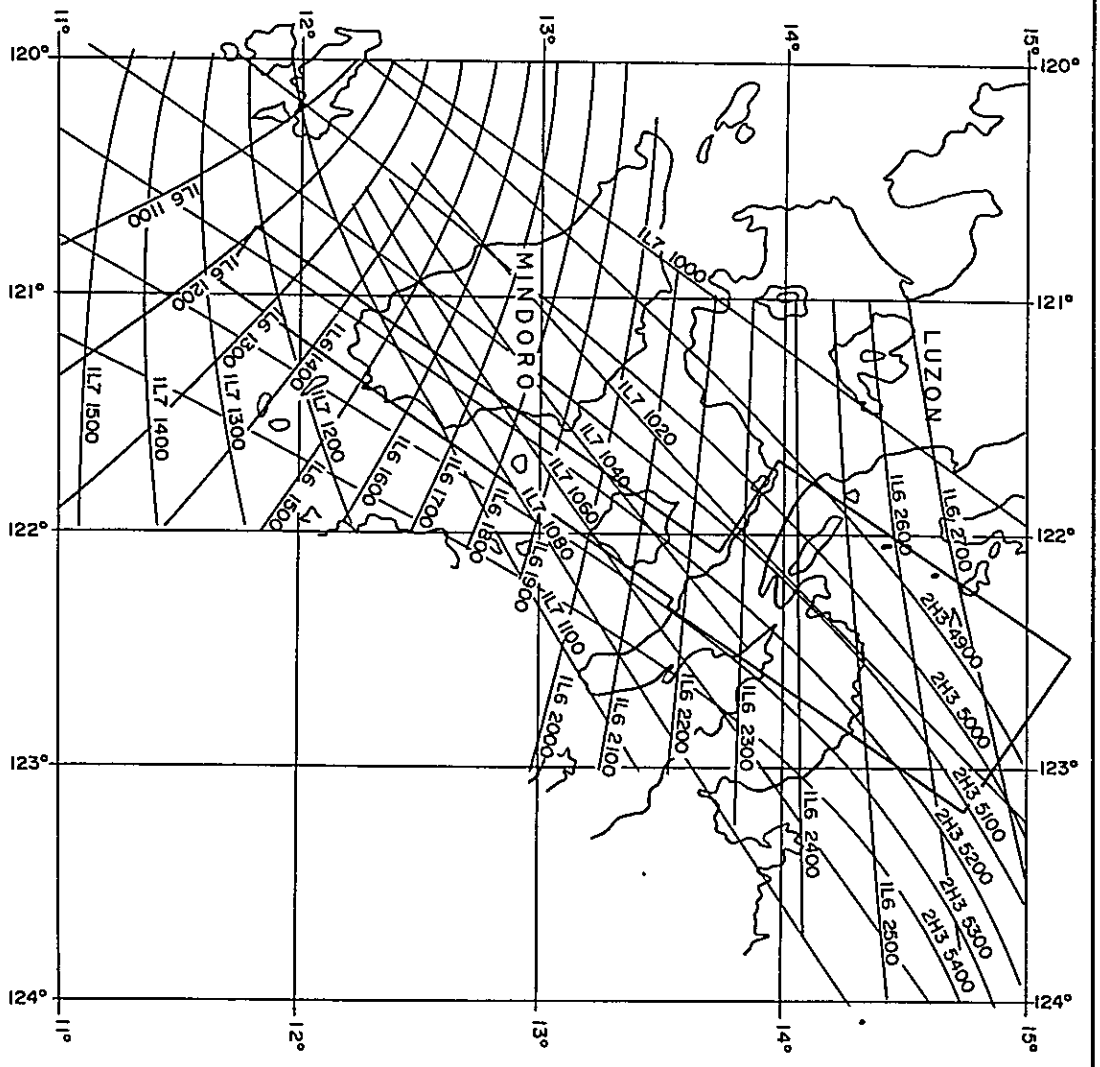

Fig.14 LORAN－A NAVIGATION CHART

MERCATOR PROJECTION

Pubhshed by the U.S. NAVAL OCEANOGRAPHIC OFFICE

became clear during the test flights that a pair of Loran-A waves from the couple 2H3 could not be received to the southwest of Bondoc Peninsula in the surveyed area. Accordingly, two couples, namely, 1L6 and 1L7 were received for the purposes of position determination and navigation.

Both groups of lines of position were considerably different in direction with the planned traverses. Therefore, straight traverses were set up independently of the curved lines of position. Navigation was carried out by instantaneous determination of the aircraft position on a topographic map with inscribed lines of position while in flight.

Besides, indication of Loran-A was photographed for permanent record by Automax-G2 pulse camera every 10 seconds.

V-4. Compilation and reduction of magnetic data

After every flight operation, the record by airborne magnetometer, film taken by streak camera and the record by station magnetometer were investigated in order to decide whether reflight would be necessary or not.

Over land areas, flight path was determined by image matching method, namely, by comparing the processed film taken by the streak camera with the air-photograph. The flight path thus determined was transfered on a topographic map at scale of 1:100,000. The streak camera used was NAC Model ST-1000. Concurrently, the flight level was shecked for deviation from a predetermined altitude by the record of a barometric altimeter. The corresponding position determined by the record of Loran-A receiver was also plotted on the topographic map so that deviation from the accurate path determined by the streak camera could be evaluated.

Over the sea, the position was determined by the record of Loran-A and plotted on the topographic map by applying the correction extrapolated from the deviation evaluated over the land areas. The flight lines were determined by connecting the plotted aircraft positions.

The positions corresponding to fiducial marks were also determined so as to transfer the magnetic records on the topographic map or the track chart. Diurnal variation of the geomagnetic field was beforehand eliminated by the following procedure. The recorded variation by station magnetometer was approximated by segments of straight line within every ± 0.5 gamma. The approximated variation of the primary magnetic field was transcribed on the corresponding part of the chart of the airborne magnetometer and subtracted from the total intensity curve. Because both the airborne and station magnetometers are not influenced by instrumental drift, the simple subtraction gives directly correction for diurnal variation.

Because only a ground magnetometer station was set up at some distance from the surveyed area, errors could occure due to the space change of duirnal variation. At the cross points of traverse and tie line, the total intensity values derived from these two observations made at defferent time might differ. Furthermore, discordane might also occure due to error of position determination. Therefore, the flight lines were adjusted so that two observations were consistent with each other at the cross points by trial and error..

The aeromagnetic records referred to the same magnetic datum were correlated with the track chart by the fiducial points. The total magnetic intensity map was subsequently completed by contouring the magnetic values indicated at the fiducil points..

Local magnetic anomalies which are embossed by eliminating regional variation are important for the aeromagnetic survey for mineral exploration. The regional variation was estimated by fitting a polynominal by means of least square to the total intensity values at the grids at a spacing of 2.5 km based on a rectangular co-ordinates.

An isogam map was drawn up from the residuals which were the difference of the total intensity from the regional variation.

The second vertical derivative and the first vertical derivative were calculated by the following formulas by using the total intensity values at the grids at a spacing of 2.5 km based on a rectangular co-ordinate system. The second vertical derivative was calculated by the following formula proposed by Rosenbach(1953):

$$\frac{\partial^2 T}{\partial Z^2} = \frac{1}{24S^2}\left(96T(0) - 72\bar{T}(S) - 32\bar{T}(\sqrt{2}S) + 8\bar{T}(\sqrt{2}S)\right),$$

where S is the grid spacing and $\bar{T}(\sqrt{n}S)$ is mean total intensity values on the grids of radius $\sqrt{n}S$. In addition, if the input of the grids on the circle of radius $\sqrt{5}S$ is not available though those on the circle of redius $\sqrt{2}S$ exist, the formula of Henderson and Zietz (1949) was used:

$$\frac{\partial^2 T}{\partial Z^2} = \frac{1}{S^2}\left(6T(0) - 8\bar{T}(S) + 2\bar{T}(\sqrt{2}S)\right).$$

The formula for the first vertical derivative is that used by Kato (1965):

$$\frac{T}{Z} = \frac{1}{S}\left(2.723T(0) - 2.885\bar{T}(S) + 0.922\bar{T}(\sqrt{2}S) - 0.760\bar{T}(\sqrt{5}S)\right).$$

The total magnetic intensity map at scale of 1:100,000 is attached as the annexed map. The isogam map, the second vertical derivative map and the first vertical derivative map were also prepared at scale of 1:250,000 and attached as the annexed maps.

VI. GEOLOGIC INTERPRETATION

VI-1. General magnetic features

The area surveyed can be divided into two zones based on the magnetic features, namely Zone A ranging from the southwestern end of the area surveyed to the western coast of Marinduque and Zone B covering the rest of the area from the western coast of Marinduque to the northwestern end of the area surveyed. In Zone A, there are a few magnetic anomalies of small amplitude and therefore, this zone is assumed to have been little influenced by igneous activities. Zone B is characterized by numerous trends of magnetic anomalies of large amplitude approximately parallel to the Philippine Rift Zone; some of the anomalies may be interpreted as being due to faults. Therefore, it is inferred that igneous activities associated with tectonic movements along definite directions were active in Zone B.

According to the geological sheet map of scale of 1: 1,000,000 (Philippine, Bureau of Mines, 1963), the igneous exposed rocks in Zone A comprise the Basement complex, Cretaceous-Paleogene intrusive rocks and Pliocene-Qraternary volcanic rocks in Mindoro. In Zone B, the Basement complex, Cretaceous-Oligocene intrusive rocks, Oligocene-Miocene volcanic rocks, Neogene intrusive rocks, Undifferentiated volcanic rocks (probably older than Paleogene), Paleogene-Eocene volcanic rocks and Pliocene-Quaternary volcanic rocks are exposed, extending approximately parallel to the direction of the Philippine Rift Zone. In Zone A, minor or deep-seated igneous activities apparently took place throughout Tertiary age, while violent igneous activities occured in Oligocene-Miocene ages in Zone B.

In view of available geologic information, the configuration of the magnetic basement configurations were interpreted in accordance with the principles described below.

(a) In Zone A, the depth of magnetic anomalies are regarded as being a direct indication of the magnetic basement on the assumption that the magnetic anomalies are mostly due to intrusive bodies of the Basement complex. The depths of the magnetic anomalies due to Cretaceous-Paleogene igneous bodies are also a likely indication of the magnetic basement. However, some anomalies are definitely identified as being due to Quaternary volcanism based on the geologic information available or on such factors as estimated depth, location in relation to known volcanic intrusions or calculated magnetic susceptibility.

(b) In Zone B, the magnetic anomalies are due not only to the igneous bodies in the Basement complex or the Cretaceous-Paleogene igneous rocks but also to the igneous bodies of later ages and accordingly, the ages of the rock formations apparently causing these anomalies had to be differentiated in order to determine the magnetic basement.

As for the land areas, first of all the type of the magnetic anomalies which correspond directly to surface geology was determined. Next, the characteristics of the neighbouring anomalies were determined to see if they should be considered to belong to the same sequence of anomalies. Among these anomalies, the surface of magnetic basement can be obtained by connecting the tops of the magnetic bodies regarded as the Basement complex or Cretaceous-Paleogene igneous rocks.

The magnetic structures beneath Marinduque Island, Bondoc Peninsula and Bicol Peninsula were determined by this means; however, the determination may not be accurate since younger volcanic rocks overlie the basement thus magnetically masking those anomalies due to the basement.

On the contrary, identification of the ages of the magnetic structures in the offshore areas, especially in the area eastward off Bicol Peninsula, was difficult because of the lack of geologic knowledge of these areas. However, it is inferred from the geology of the neighbouring land area that Neogene igneous activities were not as strong as in the Bicol Peninsula. Most of the magnetic anomalies in this offshore area may be due to igneous components of the Basement complex or to Paleocene-Encene igneous rocks. Accordingly, these magnetic anomalies should represent the magnetic basement except for those resulting from igneous bodies of later ages. Paleocene-Eocene igneous bodies are regarded as being intrusions in the basement.

Among the magnetic structures in Zone B several magnetic bodies were not correlated with the igneous components of the Basement complex nor with the Quaternary volcanic bodies. These anomalies may be considered as the indication of unconformity in sedimentary formations of Negene age.

Three examples of the subsurface sections are attached as annexed figures together with their magnetic profiles. The magnetic basement map drawn up from the results of the interpretation is also attached as an annexed map.

VI-2. Zone A

Zone A can be divided into three sub zones.

Sub Zone A_1 from the southwestern end of the area surveyed to the central part of Mindoro, characterized by a deep magnetic basement;

Sub Zone A_2 from the central part to the eastern part of Mindoro, characterized by the outcropped basement; and

Sub Zone A_3 from the eastern part of Mindoro to the western coast of Marinduque, characterized again by a deep magnetic basement.

Sub Zone A_1 is the least magnetically disturbed part of the area surveyed. Three anomalies were observed to the southwest off Mindoro. Among these three, two anomalies are extending in the northwest-southeast direction parallel to the Oriental Mindoro Fault. These three anomalies may be dur to intrusive bodies in the basement and if so, are of the intrabasement type rather than the suprabasement type.

This assumption is based on the apparent absence of major igneous activities since the Mesozoic or early Paleogene ages except for some small outcrops of younger volcanic rocks in Mindoro. Therefore, the depth of the magnetic basement is estimated from the depths of these intrabasement anomalies. The two eastern anomalies were interpreted to be dipping toward the southeast-northwest direction. Thus, the depth of the sedimentary basin increases up to 3,000 m toward the northwestern edge of the area surveyed. The center of this sedimentary basin may be about 50 km offshore to the southwest of Sanjose, Mindoro.

On the contrary, no anomalies except those due to Quaternary volcanism were observed between the above mentioned anomalies and the central part of Mindoro and no information on the basement are available. However, a sedimentary basin could exist beneath this area because in past experiences deep basins have been found to underlie such areas of no anomalies. If this speculation is true, the easternmost sequence of magnetic anomaly might indicate an eastern upheaval of the basement. Hence, two basins can be presumed to exist in Sub Zone A_1, but for one, no information of depth is available.

In Sub Zone A_2, from the central axis to the eastern coast of Mindoro, the basement is exposed over the ground surface. The basement consists of a Basement complex and Cretaceous-Paleogene undifferentiated igneous rocks with the latter being magnetic. This basement dips sharply eastward to form a sedimentary basin between Sub Zone A_2 and where it rises again toward Marinduque. This basin area comprises Sub Zone A_3, where magnetic bodies are estimated to be very deep except at the concentrated shallow anomalies around Maestre de Compo Island. These

shallow anomalies may be due to Quaternary volcanism in view of the geology of the neighbouring islands. If this assumption is correct, the magnetic basement might be the deepest around Maestre de Compo Island and would become shallower toward Marinduque. In the magnetic basement map, however, the center of the basin is shown to be located to the southeast of the area surveyed. The maximum depth may be from 2,500 to 3,000 m.

If the anomalies around Maestre de Compo Island are caused by the basement, the sedimentary basin area between Mindoro and Marinduque are separated into two basins at Maestre de Compo Island. The occurrence of this interpretation is, however, extremely rare.

VI-3. Zone B

Zone B can be divided into four sub zones:

Sub Zone B_1 from Marinduque Island to the western coast of Bondoc Peninsula including the Tayabas Isthmus;

Sub Zone B_2 from the western coast of Bondoc Peninsula to the central part of Bicol Peninsula;

Sub Zone B_3 from the central part of Bicol Peninsula to the northeastern end of the surveyed area, with the exception of Sub Zone B_4;

Sub Zone B_4 northern offshore area excluding the Tayabas Isthmus. Generally speaking, igneous activity was widespread throughout the Tertiary age except in Sub Zone B_4.

Sub Zone B_1 is characterized by many magnetic anomalies of high amplitude elongated in the northwest-southeast direction parallel to the Philippine Rift Zone. The susceptibilities of these magnetic bodies are as strong as 10^{-3} c.g.s.e.m.u. and these bodies can be correlated with Oligocene-Miocene volcanic rocks or Neogene intrusive rocks. Accordingly, the estimated depths of these anomalies do not indicate the depth of the basement and instead, correspond to the depths of Neogene igneous rocks. Even if magnetic rocks are included in the basement, these anomalies can

not be detected since the depth of the basement is greater than that of the Neogene igneous rocks.

In Marinduque, the estimated tops of the magnetic bodies are close to the ground surface. The basement must become shallower beneath this island. This interpretation is corroborated by the surface geology. The magnetic basement become deeper to the east-northeast of Marinduque down to about 1,500 m deep at the western coast of Bondoc Peninsula.

Along the northeastern coast of Marinduque, the pattern of magnetic anomaly indicates a fault in the basement, downthrown to the northeastern side and trending in the northwest-southeast direction. Parallel to the fault, another fault in the basement downthrown to the southwest side is inferred from the magnetic anomaly over Mompoc Pass between Marinduque and Bondoc Peninsula. The narrow section between these faults has no magnetic anomalies for about 10 km wide and the basement forms apparently a graben structure.

In Tayabas Isthmus, remarkable magnetic anomalies similar to those in Marinduque are distributed parallel to the Philippine Rift Zone. The magnetic anomalies can be correlated with Oligocene-Miocene volcanic rocks, Neogene intrusive rocks and the Basement complex. It was noticed that the Basement complex in this sub zone is highly magnetic.

In Sub Zone B_2, extending from the western coast of Bondoc Peninsula to the central part of Bicol Peninsula, there are two areas of no anomalies or of small amplitude anomalies; one is from the western coast to the central part of Bondoc Peninsula, and the other is from the adjoining section up to the central part of Bicol Peninsula.

No magnetic anomalies at all were observed in the former area which extends toward Ropez Bay. This is a channel of about 15 km in width. Two interpretations may be possible; one is that the basement forms a graben structure by depression along this channel; the other is that no igneous activity of Tertiary age occurred at this channel, while the basement itself was gradually undulated. The former interpretation emphasizes change in structure, whereas the latter emphasizes the defference in chemical properties. Although the magnetic anomalies not provide any means for a final conclusion, the latter interpretation was adopted.

On the other hand, the latter area is characterized by weak magnetic anomalies. These magnetic anomalies may be due to magnetic bodies near the surface, however these rocks have weak susceptibility compared with the other rocks in Sub Zones B_1 and B_2. Some of the magnetic bodies were identified to be the Basement complex based on surface geology. By tracing the sequence of magnetic anomalies, most of the magnetic bodies were considered to be a shallow Basement complex, 300 m deep at the maximum. However, the magnetic anomaly along the northeastern coast of Alabat Island in the northeastern part of this sub zone is caused by Oligocene-Miocene volcanic rocks.

The basement in this sub zone may be more than 1,500 m deep in the southwestern half where no anomalies were observed, while in the northeastern half the shallow basement associated with a fault is nearly exposed at the ground surface. The fault zone is truncated by a cleft of the fault of the surprabasement type, downthrown on the southwest side, extending from Lopez at the northwestern part of Bondoc Peninsula to Buenavista (Perez) along Ragay Gulf.

In Sub Zone B_3, there are many strong magnetic anomalies from the central part of Bicol Peninsula to the northeastern end of the surveyed area extending in a northwest-southeast direction parallel to the Philippine Rift Zone. The magnetic anomalies in the Bicol Peninsula are correlated with the igneous rocks of various ages such as the Basement complex, Undifferentiated volcanic rocks (probably older than Paleogene), Cretaceous-Paleogene intrusive rocks, Oligocene volcanic rocks,

Oligocene-Miocene volcanic rocks or Pliocene-Quaternary volcanic rocks. It should be noted that Cretaceous-Paleogene volcanic rocks widely exposed over Bicol Peninsula are strongly magnetic.

In the offshore area to the northeast of Camarines Norte Province, Bicol Peninsula, the magnetic structure could not be definitely interpreted because of lack in geologic information. Although igneous rocks of various ages may be present in this area as in Bicol Peninsula, other land areas corresponding to the offshore area are lacking in igneous rocks of the Tertiary age, especially Oligocene-Miocene volcanic rocks and in this offshore area, the Basement complex as well as Cretaceous-Paleogene volcanic rocks are exposed on Calagua Island. Accordingly, the depths of the magnetic bodies can be regarded as an indication of the magnetic basement except for the magnetic bodies indentified clearly as younger igneous bodies by tracing the sequence from the magnetic bodies of known geology. The Basement complex, Cretaceous-Paleogene volcanic rocks, Undifferentiated volcanic rocks and Oligocene volcanic rocks were regarded as being intrusions within the basement.

The magnetic basement is Sub Zone B_3 is shallow, about 500 m at most, being undulated from Camarines Norte Province, Bicol Peninsula to the northeastern end of the surveyed area, that coincides nearly with the edge of the continental shelf. However, the basement seems to be gradually dipping northeastward and is likely to be deeper beyond the margin of the outside the shelf.

Sub Zone B_4, the offshore area to be north of Bicol Peninsula and to the northeast of the Tayabas Isthmus is characterized by three great magnetic anomalies of large wave lengths which may suggest a sedimentary basin increasing its depth northward. These three anomalies are located in the vicinity of Bacesin Island, about 15 km to the south of Jomalig Island and around Patnanongan Island.

These magnetic anomalies are of the intrabasement type, due to wide intrusive bodies of which the depths are estimated to be about 3,000 m. The center of this sedimentary basin may be located at the edge of the area surveyed or some place northwestward outside the area. Nevertheless, this basin may not be so broad because the Basement complex is exposed at Polillo Island to the northwest of this basin.

VII. CONCLUSION

Since little subsurface information such as data of drilling or seismic surveys are available, the magnetic basement map shows merely a possible solution and reinterpretation is recommended when more information becomes available.

The present survey was a reconnaissance and consequently, the traverses were so widely spaced that small subsurface structures might have been overlooked. However, since the traverses are perpendicular to the main geologic trend, the chances of missing such small structures were minimal and the accuracy of this quantitative interpretation can be accepted with a certain level of confidence.

In the area surveyed, the magnetic anomalies are likely caused by a difference in the chemical composition of the basement; in other words by igneous bodies in the basement. The application of an intrabasement model is favourable for this interpretation rather than suprabasement model since otherwise, only a few anomalies would be pertinently interpreted. This is the reason that model matching methods were used instead of the methods based on a two-layered structure. Therefore it was inevitable that this methods could not obtain information on the basement depth in the areas lacking intrabasement type anomalies.

Several sedimentary basins were recognized in the offshore areas, although they are not extensive. These sedimentary basins may have hydrocarbon potential. Many igneous intrusions were observed and those on land were correlated with igenous rocks of various ages associated with tectonic movements. Mineralization could be associated with these igneous bodies.

Among the several basins revealed by the present survey, the basins south of Mindoro and the one in Lamon Bay may be more attractive for petroleum prospecting than the others, since they are apparently contain thicker sections of

sediments. Unfortunately, the total mileage was so limited that these basins were not fully covered by the present survey. Further investigations of these basins are higly desirable by such a geophysical method as reconnaissance seismic profiling as well as by detailed surveys of the island's geology.

REFERENCES

Alcaraz, A.P., 1947, The major structural lines of the Philippines:
The Philippine Geologist, vol. 1, no.2, p.13-17.

Bhattacharia, B.K., 1965, Two-dimensional harmonic analysis as a tool for magnetic interpretation:
Geophysics, vol. XXX, no.5, p.829-857.

Chastenet De Gery, J. et H. Naudy, 1957, Sur l'interpretation des anomalies gravimetriques et magnetiques:
Geophysical Prospecting, vol. 5, no.4, p.421-448.

Corby, G.W. et al., 1951, Geology and oil possibilities of the Philippines:
Tech. Bull., Philippine Bureau of Mines, 21, Manila, pp.363.

Feliciano, J.M. and D.M. Basco, 1947, Preliminary geologic report of the Mansalay district, Mindoro:
The Philippine Geologist, vol. 1, no.3, p.1-11.

Frost, J.E., 1959, Notes on the genesis of the ore-bearing structures of the Paracale district, Camarines Norte, Philippines:
The Philippine Geologist, vol. XIII, no. 2, p.31-43.

Gay Jr., S.P., 1963, Standard curves for interpretation of magnetic anomalies over long tabular bodies:
Geophysics, vol.28 no.2, p.161-200.

Gervasio, F.C., 1958, The geologic structure of Marinduque Province and their relation to ore localization:
The Philippines Geologist, vol.XII, no.3, p.85-90.

, 1966a, A study of the tectonics of the Philippine archipelago:
The Philippine Geologist, vol.XX, no.3, p.51-75.

, 1966b, The age and nature of orogenesis of the Philippines:
The Philippine Geologist, vol.XX, no.4, p.121-140.

Giret, R. et H. Naudy, 1963, Methods actuelles d'interpretation des etudes aeromagnetiques en recherehe petroliere:
The Sixth World Petroleum Congress, Section 1, Paper 15-PD4.

Grant, P.S and L. Martin, 1966, Interpretation of aeromagnetic anomalies by use of characteristic curves:
Geophysics, vol.31, no.1, p.135-148.

Hahn, A., 1965, Two applications of Fourier's analysis for the interpretation of geomagnetic anomalies:
Jour. Geomag. & Geoelect., vol.17, no.3-4. p.195-225.

Henderson, R.C. and I. Zietz, 1949, Computation of second derivative of geomagnetic field:
Geophysics, vol.14, no.4, p.508-516.

Kato, M., 1965, Generalized treatments of sampling filter (in Japanese) :
Butsuri Tanko (Geophysical Exploration), vol.18, no.1, p.1-13.

Moo, J.K.C., 1965, Analytical aeromagnetic interpretation, the inclined prism:
Geophysical Prospecting, vol.13, no.2, p.203-224.

Nagata, T., 1938, Magnetic anomalies and the corresponding subterranean mass distribution:
Bull. Earthq. Res. Inst., vol.16, p.550-557.

Petroleum Division, Philippine Bureau of Mines, 1970, General geology of Paracale mineral district, Camarines Norte, Marinduque Island and Southern Mindoro:
unpublished report, pp.6.

Philippine Bureau of Mines, 1963, City of Manila(ND-51):
Geological Map Series, millionth scale, Manila.

Rosenbach, 0., 1953, A contribution to the computation of the "second derivative" from gravity data:
Geophysics, vol.18, no.4, p.894-909.

Santos-Ynigo, L.M., 1959, Geology of the copper-molybdenum deposits at Tumbagahan, Boac, Marinduque:
The Philippine Geologist, vol.XIII, no.2, p.62-77.

, 1966, Island arc structures of the Philippine archipelago:
The Philippine Geologist, vol.XX, no.3, p.79-92.

Segawa, J., 1967, A method of determining subterranean anomalous structure from the distribution of local anomaly in geomagnetic total force:
Jour. Geodetic Soc. Japan, vol.13, no.1, p.20-44.

Tsuboi, C. and T. Fuchida, 1937, Relations between gravity values and corresponding subterranean mass distrubution:
Bull. Earthq. Res. Inst., vol. 15, p.636-657.

Vacquir, V. et al., 1951, Interpretation of aeromagnetic maps:
Memoir 47, Geological Society of America.

Weller, J.M. and J.F. Vergara, 1955, Geology and coal resources of the Bulalacao region, Mindoro Orental:
Special Project series, Publication no.1 - Coal, Philippine Bureau of Mines, Manila, pp.37.

APPENDIX I SPECIFICATIONS AND STATISTICS

Aircraft	:	YS11, prop-jet, twin-engined.
Airbase	:	Manila.
Duration of survey flight	:	12 - 27 March, 1970
Flight altitude	:	3,000 ft from the sea level except mountaneous area.
Airspeed of aircraft	:	140 knot. (about 150 knot in ground speed)
Magnetometer	:	Varian Model V 4914 Proton Airbone Magnetometer. Varian Model V 4938G Cesium and Rubidium Ground Magnetometers.
Aerial Camera	:	NAC Model ST-1000 Streak Camera.
Altimeter	:	Barometric.
Navigation	:	Furuno Electric Model LK-12 Loran-A Receiver.
Scale of aeromagnetic maps	:	Total Magnetic Intensity - 1 : 100,000. Isogam, Second Vertical Derivative, First Vertical Derivative and Magnetic Basement - 1 : 250,000.
Direction of traverses:	:	approximately N 35^{o} W.
Spacing of traverse lines	:	6 km, occasionally 12 km.
Traverse line length	:	6 long traverse lines, 460 - 320 km. 8 short traverse lines, 135 km - 35 km.
Tie line length	:	5 lines, 100 km - 50 km.
Total flight line length	:	4,400 line-km.
Total traverse line length	:	4,000 line-km including reflight of 200 line-km.
Total tie line length	:	400 line-km.
Total area surveyed	:	18,500 sq. km.
Total flight hours	:	44h 40 m excluding taxing.

Total fuel consumptions	:	13,001 U.S. galons (kerosene).
Inclination of geomagnetic field	:	15°N.
Total intensity of geomagnetic field	:	40,000 gamma.

APPENDIX II MAGNETIC PROPERTIES OF ROCK SAMPLES

During the preliminary investigation made by the Japanese expert team sent to the Philippines from March to April, 1968, 23 rock samples were collected. The magnetic properties of these samples were measured for comparison with the interpretations of the aeromagnetic survey. Fig. A-1 shows the localities of the samples and Tab. A-1 presents the results of the measurement. Some of the samples were collected outside the surveyed area.

Intensity of induced magnetization was measured by a susceptimeter made by the Japan Petoroleum Exploration Co., Ltd. based on the alternating current method. The effective magnetic field was 0.4 Oe. and the frequency was 1,000 Hz. The sensitivity was 10^{-6} c.g.s.e.m.u., while the accuracy was three digits. Intensity of natural remnant magnetization was measured by an astatic magnetometer made by Sokkisha, Ltd. The sensitivity was 10^{-5} c.g.s.e.m.u., while the accuracy was three digits.

The number of the samples was not enough for reaching a definite conclusion. The results agree with the general characteristic of rock magnetism, namely, ultrabasic rock, basic rock, acidic rock and sedimentary rock in the order of decreasing magnetization.

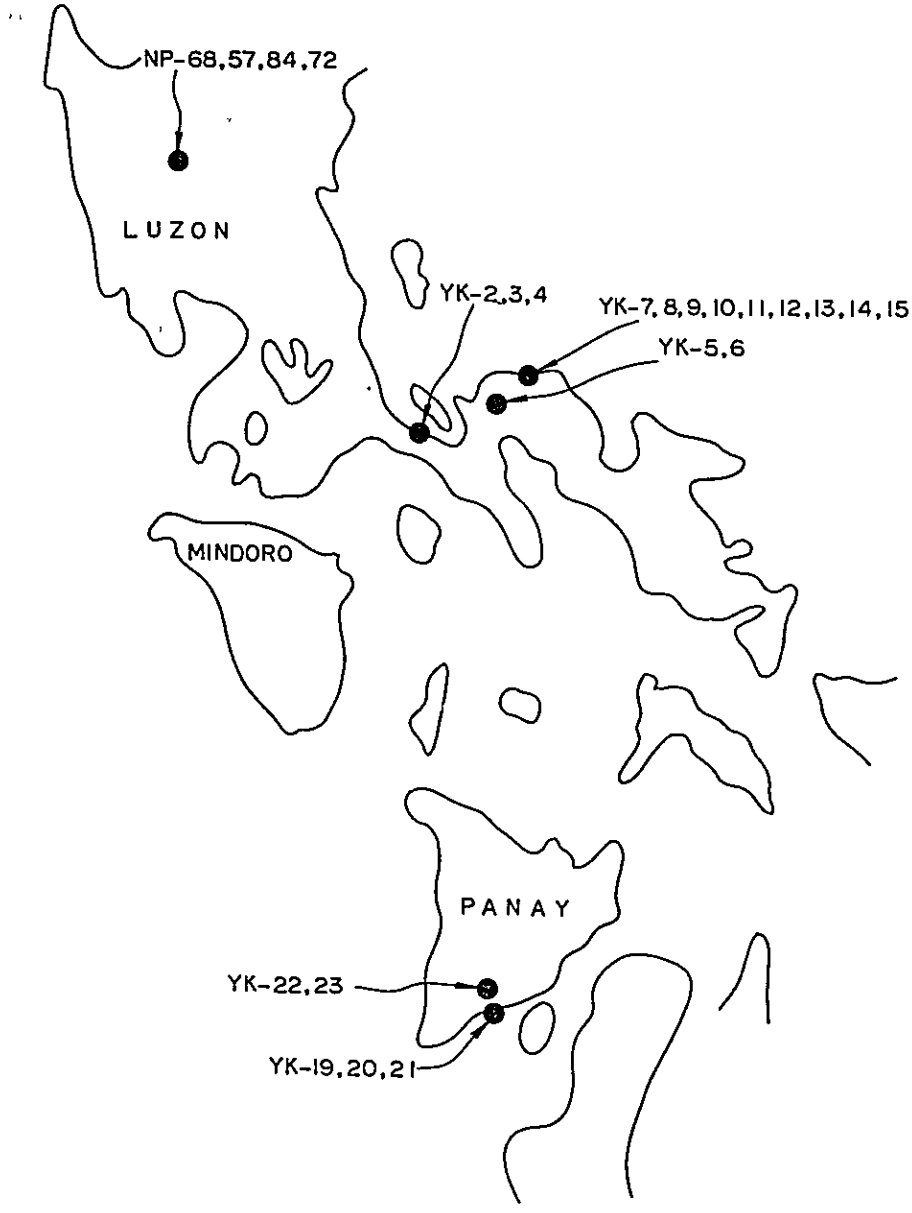

Fig. A-1 Localities of the rock samples

Tab. A-1. (a) Localities and rock types of the samples

No.	Locality	Rock type
YK 2	San Isidoro (Quezon)	Basement complex
YK 3	"	"
YK 4	"	"
YK 5	Negritos Camp (Camarines Norte)	Serpentine
YK 6	"	Peridotite
YK 7	Larap (Camarines Norte)	Syenite
YK 8	"	Peridotite
YK 9	"	Granite gneiss
YK 10	"	Tertiary igneous
YK 12	"	Diorite
YK 13	"	Andesite
YK 14	"	"
YK 15	"	"
YK 19	Sawaragan (Panay Island)	Tuff (Mesozoic agglomerate)
YK 20	"	Basalt (")
YK 21	"	Tuff (")
YK 22	Tallas River (Panay Island)	Olivine basalt
YK 23	"	"
NP 68	Talrac (Talrac)	Shale
NP 57	"	"
NP 84	"	Sandstone
NP 72	"	Shale

Tab. A-2 (b) Magnetic properties of the samples

No.	Density	Susceptibility	Intensity of "IM"	Intensity of "NRM"	Declination of "NMR"	Inclination of "NRM"	Ratio
	ρ g/cm^3	K cgsemu	J_i emu/cm^3	J_r emu/cm^3	φ degree	θ degree	J_r/J_i
YK 2	2.62	2.1×10^{-5}	8×10^{-6}	0×10^{-5}			0
YK 3	2.66	8×10^{-6}	3×10^{-6}	0×10^{-5}			0
YK 4	2.62	1.54×10^{-3}	6.16×10^{-4}	4.4×10^{-4}	157°	58°	0.71
YK 5	2.76	1.31×10^{-3}	5.24×10^{-4}	5×10^{-5}	0°	26°	0.09
YK 6	2.68	3.8×10^{-5}	1.5×10^{-5}	0×10^{-5}			0
YK 7	2.73	8.24×10^{-3}	3.30×10^{-3}	1.12×10^{-3}	51°	0°	0.34
YK 8	2.58	2.71×10^{-3}	8.40×10^{-3}	8.40×10^{-3}	312°	9°	7.78
YK 9	2.50	1.65×10^{-4}	6.6×10^{-5}	0×10^{-5}			0
YK 10	2.69	8×10^{-6}	3×10^{-6}	0×10^{-5}			0
YK 11	2.51	8×10^{-6}	3×10^{-6}	0×10^{-5}			0
YK 12	2.67	4.30×10^{-3}	1.72×10^{-3}	6.5×10^{-4}	149°	28°	0.38
YK 13	2.53	1.0×10^{-5}	4×10^{-6}	0×10^{-5}			0
YK 14	2.25	2.77×10^{-3}	1.11×10^{-3}	4.64×10^{-3}	57°	49°	4.18
YK 15	2.84	4.75×10^{-3}	1.90×10^{-3}	1.62×10^{-3}	343°	51°	0.85
YK 19	2.20	4.51×10^{-4}	2.14×10^{-4}	2.2×10^{-4}	349°	-16°	1.03
YK 20	2.46	2.85×10^{-4}	1.14×10^{-4}	8.8×10^{-4}	319°	-9°	7.72
YK 21	2.36	3.07×10^{-4}	1.23×10^{-4}	1.4×10^{-4}	51°	-20°	1.13
YK 22	2.48	8.90×10^{-3}	3.56×10^{-3}	0×10^{-5}			0
YK 23	2.70	4.81×10^{-3}	1.92×10^{-3}	1.94×10^{-3}	244°	33°	1.01
NP 68	2.58	4.4×10^{-5}	1.8×10^{-5}	0×10^{-5}			0
NP 57	1.69	0×10^{-6}	0×10^{-6}	0×10^{-5}			0
NP 84	2.56	0×10^{-6}	0×10^{-6}	0×10^{-5}			0
NP 72	2.61	6.8×10^{-5}	2.7×10^{-5}	0×10^{-5}			0

H = 0.4 Oe.